

An Integral View of the Hydrographic Development in the Greenland Sea Over a Decade

G. Budéus* and S. Ronski

Alfred-Wegener-Institut for Polar and Marine Research, Columbusstr., 27568 Bremerhaven, Germany

Abstract: A thirteen year long time series (1993 to 2005) of basin wide transects is used to analyse the hydrographic development in the Greenland Sea and to identify the processes which are responsible for observed changes. A key feature is the structural change away from a cold water dome to a two layer structure which is related to a fresh water convergence around 1990. The ensuing changes in the upper layer, the interface, and the lower layer are discussed in detail. The upper layer increases continuously in volume and shows no unequivocal trend in any hydrographic property. All observed modifications are reversible. The interface descends steadily with time by more than 1000 m during the investigation and shows constant properties. At the end of the time series, the deep layer volume is reduced to only 50% due to the interface descent. Both temperature and salinity show unambiguous trends in this layer. The temperature increase is mainly caused by vertical advection, the salinity increase by exchange with deep Arctic waters. The observations corroborate the idea that a large single-cell continuous convection scheme dominates the volume changes of both upper and lower layer and the deep water modifications during the 90s. These changes are independent of winter convection. The export from the deep layer is concentrated at the western continental slope of the basin.

1. INTRODUCTION

The region between Fram Strait and Jan Mayen attains increased scientific attention during the recent few decades due to a number of key properties. The atmosphere ocean transfers of momentum, heat and freshwater are strong, particularly during the cold winter months. Water masses from low and high latitudes meet and interact by means of mixing at fronts, subduction, entrainment, and winter convection. Sea ice is formed in the northern and western parts and is transported southward with the cold and fresh surface waters in the East Greenland Current (EGC). Dense waters are formed which act as a major contribution to the Atlantic Meridional Overturning Circulation or as the source of deep Arctic Waters. All this makes the region highly sensitive to climatic changes and also leads to feedback mechanisms which vice versa affect the north European climate. Investigations of such large scale climatic aspects must evidently be based on sound perceptions of local modifications.

A delineation of the temporal development in the central Greenland Sea seems to be a gratifying task, as it is obvious that frequency, thoroughness and accuracy of field measurements have developed enormously since the late 80s. Various large projects have been conducted (ESOP (European Subpolar Ocean Programme), [1]), CONVECTION (Greenland Sea convection mechanisms and their climatic implications), TRACTOR (Tracer and Circulation in the Nordic Seas)), including a multitude of innovative approaches as e.g. the SF-6 deployment [2,3] and drifter programmes. It is self evident that these enhanced research activities during the

90s reveal a much more adequate and detailed description of status, trends and main processes in every part of the Greenland Sea than has been available before.

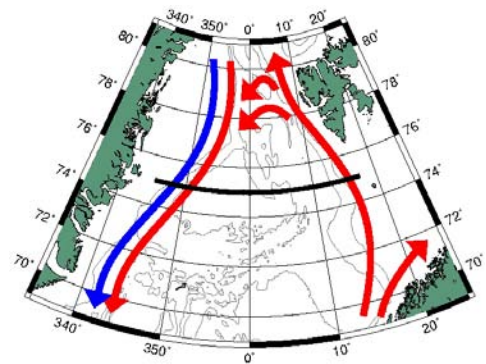


Fig. (1). The Greenland Sea area with Greenland (left), Svalbard (upper right), and the northern part of Norway (lower right). The zonal transect is marked in black. Prominent surface currents are shown in red (warm) and blue (cold).

With a closer look it is quickly evident, however, that these activities do not result in a straightforward and consistent time series which reveals the complete body of relevant hydrographic processes. Specialised research interests often lead to specific measurement strategies and different spatial extents, and often station grid patterns have been employed which vary from cruise to cruise. Many times measurements include only part of the ocean's full depth due to time constraints. For these reasons we rely here mainly on our own 10 year data set of a zonal transect across the Greenland Gyre and make no attempt for a complete review including as many field data as possible. This has the advantage of well

*Address correspondence to this author at the Alfred-Wegener-Institut for Polar and Marine Research, Columbusstr., 27568 Bremerhaven, Germany; E-mail: gbudeus@awi-bremerhaven.de

known and documented correction procedures which are mostly unavailable for published data sets but are important with respect to the partly small property differences discussed - in time as well as in space - and also with respect to the finding that local variability is often similar to or larger than the seasonal one.

While many aspects of the internal circulation and of convection processes turned out to work differently than thought before, certain parts of the general setting of the region are persistent and well established. Main features are sketched, somewhat simplified, in Fig. (1). At the eastern rim of the basin, the warm waters of Atlantic origin move northward as a 600 - 800 m thick layer in the West Spitsbergen Current (WSC). Recent observations show that their average velocity is slow, while local speeds are not [4]. The western boundary of the Atlantic Water (AW) forms a sharp temperature and salinity front which is less pronounced in density [5,6]. Numerous eddies form and detach from this front with associated lateral exchanges [6,7]. The large scale meridional flow serves as the most important heat supply for the Arctic, although substantial portions of the waters recirculate already in Fram Strait [8-10]. In this region, the AWs meet the lighter Polar Waters heading southward, and, together with deeper waters from the Arctic, they form the EGC. The sill depth in Fram Strait limits the downmost extent of the exiting Deep Polar Waters to about 2600 m. The EGC is much narrower than the West Spitsbergen Current but transports similar water volumes, and, most relevant for the fresh water and heat balance, carries with it also the melting pack ice cover.

The huge cold water dome in the central Greenland Sea has been identified by [11] already in the early decades of the 20th century (by cruises between 1901 and 1905). Since then, the doming of deep water temperatures between the warm rim currents has been regarded as synonymous to the regular occurrence of local deep and bottom water formation. In the 80s, this idea has been revised towards the cognition that bottom water formation by surface forcing is a rather rare process but must occur occasionally [12,13].

In this paper we will delineate the hydrographic development during the last decade on a basin wide scale and identify the processes which are responsible for observed changes. The approach is based on field observations. As we rely on our own 10 year data set we evidently exclude previous trends (in the 80s) from the discussion and analysis. Our transect, with all stations performed to full ocean depth, is executed once per year and extends from the shelf off Bear Island to that of East Greenland, including the area covered with pack ice. Therefore it includes the water masses at the rims and allows to determine lateral gradients not only in the interior of the Greenland Basin but also towards the water mass end members. This spatial information is essential with respect to a correct perception of advectively caused modifications as e.g. the influence of the deep Arctic outflows. We also employ small station distances in order to obtain a sufficient number of stations which allows to discriminate between spatial and temporal differences. It will be seen, that the annual expeditions represent a very adequate approach for the determination of the multi year development and its underlying processes, while seasonal changes do evidently not fall under the scope of this paper. On the other hand, the

annual resolution is a minimum observation frequency, as comparisons of snapshots which are several years apart are mostly adverse to a correct process related interpretation.

MATERIAL AND METHODS

Data

An overview over the performed cruises and the employed equipment is given in Table 1. For the CTD-work in 1993, the WOCE (World Ocean Circulation Experiment) approved Neill Brown MkIII was used. To gain smooth data, appropriate bin sizes have been chosen for this year (5 dbar). The data have been treated as an entity with respect to conductivity and temperature corrections, as opposed to a method of individual fits between single station's data to bottle data or other reference values.

Since 1994, data quality is essentially consistent, as the same or similar equipment has been used (SBE 911+). During the more recent years, the same sensors have been used during all cruises. In common for all cruises, laboratory calibrations have been performed immediately before and after each cruise (the differences between pre- and post-cruise calibrations are included in the Table 1). Duplicate sensor sets have always been mounted and their differences have been evaluated immediately in order to check for possible sensor drifts or fouling problems already on board of the research vessel. Vertical bin size is 1 dbar. Despite the overall consistent quality, methodological improvements with time are apparent also after 1994. The electrical reference thermometer SBE35, which is a more precise reference thermometer (SBE 35) than available before, has been used since 1996 for in-situ comparisons against the sensors. Such comparisons serve essentially as one point calibration checks and cannot replace laboratory calibrations but they are useful to detect possible pressure effects on the thermometer in the mK-range (compare [14]). A small pressure dependence of one of the routinely used temperature sensors (S/N 1338) of about 1 mK/4000 dbar could only be identified with the advent of this reference. This cross dependence is regarded as a sensor characteristic and the same linear term has been used throughout all cruises to correct it. For in-situ calibration checks in the Millikelvin-range one has to investigate carefully whether an in-situ comparison between CTD sensors and a reference thermometer is allowed. Surprisingly, this is not the case for most parts of the transect across the Greenland Sea including the deep waters. Post cruise temperature corrections in our time series are performed as offsets to the entire data set.

Some of the corrections have been applied very hesitantly. This is particularly true for the temperature correction in 2000 and 2001, where comparisons between the SBE3 CTD temperature sensors and the SBE35 reference showed differences of about 1.5 mK, while pre- and post-cruise calibrations of the CTD sensors revealed no drift of similar magnitude. Despite this, the SBE35 values have been regarded as valid references during these years. Later, we abstained from corrections when no sensor drift was apparent. The mentioned corrections may be regarded as the present limit of calibration and field measurement accuracies, and luckily these are an order of magnitude smaller than the observed annual temporal difference e.g. in the bottom water

Table 1. Cruise and Sensor Details. NB Denotes Neill Brown CTD. Temperature Drift and Correction are Given in mK, Drift is the Difference between Pre- and Post-Cruise Calibrations. Salinity Correction is Given in 1/1000

Year	Ship	Month	Temp Sensor	Temp Drift	Temp Correct.	Cond Sensor	Sal Correct.
1993	Polarstern	Apr	NB	n/a	-2.2	NB	f(p,T,C)
1994	Polarstern	Jul	1488 1491	9. 0.25	- 0.	1198 1199	- 2.
1995	Polarstern	Oct	1491 1488	-0.4 -0.1	0. 0.	1199 1198	9. 9.
1996	Petr Kottsov	Sep	1338 1488	0.0 -0.2	0. 0.	1198 1199	2. 2.
1997	Polarstern	Sep	1491 1338	0.2 0.0	0. 0.	1198 1199	0. 0.
1998	Polarstern	Sep	1491 1632	0.1 n/a	0.5 -7.	1199 1493	0. 0.
1999	Polarstern	Jul	1491 1338	0.7 0.6	-1. 0.	1198 1199	0. 0.
2000	Polarstern	Jul	1491 1338	0.3 -1.2	-1.5 -1.5	1198 1199	0.5 0.5
2001	Polarstern	Jun	1491 1338	0.9 -0.4	-1.5 -1.5	1198 1199	-1.5 -1.5
2002	Polarstern	Oct	1338 1491	0.2 0.4	0. 0.	1199 1198	2. 2.
2003	Polarstern	Apr	1338 1491	0.4 1.2	0. 0.	1199 1198	-6. -
2004	Polarstern	Jul	1338 1491	-0.2 -0.1	0. 0.	1199 1198	-3. -3.
2005	Polarstern	Aug	1338 1491	2.3 0.8	0. 0.	1199 1198	-4. -4.

temperatures of the Greenland Gyre, so that the latter is still well resolved.

With respect to salinity accuracies, the problems are less well settled. The salinity standard is comprised of two elements: the standard water itself and the Guildline Autosal salinometer. The latter is very sensitive to trends and fluctuations of the ambient air temperature, it induces unnecessary changes of its internal water bath temperature if samples are not perfectly temperature equilibrated before they are evaluated, and there is no indication whether measurements are allowed in a certain moment or not. Its accuracy specification is 0.003 in salinity, and as we take this as a serious statement, we cannot claim for a higher final accuracy of the field data.

Consequently, it may be astonishing that salinity or conductivity corrections of smaller magnitudes are applied. The reason is as follows and essentially based on field evidence: It serves as a basic presumption that salinity in the bottom waters of the Greenland Basin (west of about 0°E) cannot decrease, as no mechanism is known or even discussed which might reduce the bottom water salinities there under the absence of deep winter convection. Thus, we take the

1993 cruise, during which a very extensive bottle sample evaluation has been carried out (N. Verch, IfM Hamburg) as a starting point and prohibit a salinity decrease in the subsequent years.

As for the temperature corrections, all post cruise adjustments are applied to the entirety of a cruise's salinity or conductivity measurements. The corrections are applied as offsets or simple factors and do not contain cross dependencies on temperature or pressure. (Due to the different equipment used, the 1993 data set is an exception from this.) As all corrections are specified, it is easy to revise them if future field results reveal evidence for such a need. Of course, the described method is methodologically not fully satisfying, since it presumes certain properties of a subject which is itself object of ongoing research; however, it seems to be the best we can do at present. Corrections which have been applied for each cruise are also included in Table 1.

Proprietary processing software from Sea-Bird Electronics has been applied when the SBE911+ CTD has been used (i.e. after 1993). The applied routines include *datcnv*, *alignctd* (with individually optimised time shifts for each cruise and sensor set), *celltm* (nominal values used), *loope-*

dit, filter (150 ms on pressure), and binavg, resulting in 1 dbar bins of the original parameters. Subsequent calculations are performed by in house software according to EOS80. The Hesselberg stability parameter

$$E = -\frac{1}{\rho} \frac{\partial \rho}{\partial z} - \frac{g}{C^2} \quad (\text{with in situ density } \rho)$$

is used to characterise the vertical stability. Regional means of all parameters are based on averages of 6 profiles per year which are located immediately west of zero degrees and coherent vortices (CVs) are excluded as these deviate greatly from the background conditions and represent only a very small volume (compare separate chapter below). Restrictions with respect to the regional coverage had to be accepted only in 1996, when the used ship could not access waters under Danish administration.

Transect Plots

It poses a continuous problem to produce intelligible and correct contour plots when trying to depict oceanographic data. Much of the problem arises from the two facts that oceanographic stations are usually not performed on a regular grid, and that vertical resolution (order of 1 dbar) exceeds horizontal resolution (many nautical miles) by several orders.

The solution used here is born from the consideration that the most essential demand for the scientific interpretation of a data visualization like a contour plot is to conserve the measured data at the respective stations and avoid plot artefacts which are not covered by measurements. We achieve this by relatively simple means. We control interpolation and inhibit extrapolation in the following way, which establishes a regular data grid that can easily be plotted: On the transect, the minimum station distance is identified, and all other distances are interpreted as integer multiples of this minimum. Where necessary, one or more additional profiles are introduced by strictly horizontal interpolation of the two neighbouring profiles. Thereafter, the total length of this transect is checked, and if it differs less than 10% from the real transect length, plotting is performed. If this margin is exceeded, the minimum station distance is divided by two, and again all station distances are interpreted as integer multiples. This is repeated until the error of the plotted transect length is within the mentioned 10%. Normally, one or two steps suffice to achieve this for our transects.

While the location of a certain station in the plot might therefore not correspond exactly to its position on the real transect (which seems to be a minor fault because no calculations are done from the plot), the measured quantities are exactly conserved at all stations and are positioned exactly at the station tick mark (with the advantage that data checking is also facilitated). There are no artificial isolated extrema at locations where no data have been sampled, and the maximum vertical excursion of the isopleths is always found at a station. Despite of the major advantages of the applied method it is not without minor drawbacks. The first is that at slopes of the ocean bottom the triangle which is not covered by the vertical extent of both neighbouring stations is not filled because extrapolation is inhibited. Resulting from the same effect, but more serious, is that the deepest station in a trough is not depicted to its full depth but only to that which

it has in common with its neighbours. Here, an inspection of the original data file, whether by other plots like profiles or TS-diagrams or by checking the data listing, is the only solution in our context.

The transect figures contain the three basic hydrographic parameters potential temperature θ , salinity, and potential density σ_θ for the entire set of observations. These figures are also included on a CD containing the complete data set (available from the authors). For comparison, a transect from [15] which was performed on a comparable route (NW to SE) in 1982 is also presented in the same format and with the same class limits. Please note that class limits are not equidistant, because this is the only way to allow for a recognition of all important features. However, the class limits are kept constant throughout the shown period. The transect contour plots from 1993 to 2005 are shown in Fig. (2) (potential temperature), 3 (salinity), 4 (density), and the situation of the early 80s in Fig. (5).

MAIN FEATURES

The main features observed in the transects are introduced in this chapter as an overview of the general hydrographic structure of the Greenland Sea in the 90s. As the transects extend from close to the Greenland coast (left side) to Bear Island on the Barents Shelf (right side), the observations include not only the hydrographic conditions in the central Greenland Gyre but also those of the source water masses at the rims, and we envisage them first.

The northward flowing Atlantic Waters in the eastern part of the transect are marked by high temperatures and salinities. The main body of the Atlantic Water extends to roughly 5°E and shows a thickness of 600 to 800 m. The western limit of the AW forms the so called Arctic Front. It is often structured in a way that indicates eddy activity and exchange across the front (see isolated high salinity patches west of the front e.g. in 1994, 1996, 1997 ff). The details of the front are apparent in the temperature and salinity distribution, but are not mirrored in the density field.

In the western part, the southward flowing Return Atlantic Waters (RAW), which are included in the East Greenland Current, form a local temperature and salinity maximum. The RAWs meet the continental slope at depths between 200 and 400 m and approach the surface further to the east. There is no special term assigned to the eastern limit of RAW, although it forms an important boundary. Similar to the AW limit in the eastern part of the basin, the limit of the RAW is full of structure which is hardly visible in the density field. Detached RAW patches are often found far away from the RAW/EGC core (e.g. 1994, 1995, 1999, 2001, etc.). The western limit of the RAW, the so called East Greenland Polar Front, which separates the RAW from the much fresher and colder Polar Water (PW) is clearly visible in the temperature, salinity and density fields. The PWs include a large variety of sources [16,17] and carry the Arctic pack ice with them. Their main body is confined to the shelf, but they do spread as a thin surface layer over the RAW in summer and form a temporal low salinity top layer throughout the Greenland Basin.

In the 80s, the area between the two streams of Atlantic Waters was occupied by a cold dome structure (Fig. 5, data

from [15]). This is not the case during the 90s. A major structural change occurred which is far beyond a gradual shift of properties. In contrast to the former cold dome, the vertical structure in the central basin consists of two main layers during the 90s: an upper layer and a lower layer which are separated by a distinct interface. The upper layer contains a lens of relatively cold ($\theta < -0.85^\circ\text{C}$) and fresh ($S < 34.89$) waters. Winter convection affects this layer which extends during winter to the surface (see cruise in April 1993). The temporal development of the temperature, salinity and stability fields and the related exchange processes will be discussed later in detail. The layer is limited vertically by a pronounced salinity and σ_θ gradient which is accompanied by a local vertical temperature maximum (intermediate temperature maximum). This interface between the upper and lower layer descends with time while its properties remain constant within a very small range. Occasionally, the interface seems to be locally disrupted and penetrated from above by eddies (Coherent Vortices, CV [18-20]), but a closer inspection reveals that the interface is only displaced downward and slightly eroded at these CV sites. CVs can be recognised in the transect plots in 1993, 1994, 1997, 2001, and 2002 and show a colder, less saline, and more homogeneous core in comparison to their upper layer surroundings. In summary, the upper layer of the Greenland Basin is bounded by warmer and more saline waters everywhere today, in the vertical as well as in the horizontal. Its relative temperature and salinity minimum points to winter convection as its characteristic formation mechanism.

The lower layer in the Greenland Basin contains the remaining waters of the former cold dome. Below the interface, temperatures decrease steadily towards the ocean bottom, where the coldest deep waters are found. Local winter convection in the past is the only explanation for the cold bottom waters. However, the volume below the interface continuously decreases (the interface is found at 1000 m in 1993, but at 1800 m in 2003) and the coldest temperatures disappear steadily. In the mentioned 10 year period, the potential temperatures in the coldest waters at the bottom increase from -1.20 to -1.10°C . The transect plots show the volume reduction and disappearance of several temperature classes clearly.

The salinity in the deep layer is increasing continuously throughout the presented observation period, and the disappearance of several low salinity classes can be recognised in the transect plots. Already in 1993 there is almost no water left that retains the properties of the classical 'Greenland Sea Deep Water' with salinities below 34.90. The source for the salinity increase is immediately obvious from the transects: it is fed by the deep Arctic outflow. As this surrounds the Greenland Basin - ideally revealing a rotational symmetric structure - the salt input into the deep Greenland Sea waters occurs from all along its circular boundary.

UPPER LAYER DEVELOPMENT

The upper layer's volume increases with time because the interface to the lower layer descends in the course of the time series; thus, a fixed depth limit is not applicable to the layer. The varying depth of the salinity/density gradient with the associated temperature maximum is used here as its lower limit. We take the surface as its upper limit because

various physical processes affect it as an entity. The layer is open to the surface during the convection phase (compare 1993, when the cruise was performed in March/April, Fig. 2a) and often winter convection affects it down to the interface. Advective influences and exchange with the rims occur at all its depth levels. The advective signal is most pronounced close to the surface, where Polar Waters (upper few 10 metres) and Atlantic Water derivatives (immediately below the PW, but extending to variable depths) are imported.

Winter convection mixes the combined imports to greater depths, thus 'resetting' the hydrographic status of the upper layer. Above the maximum convection depth, the advective signal proceeds after winter from a new state, while below the maximum convection depth it continues uninterrupted. Both PW and AW contributions are quite variable in time and space. Considerable interannual differences of their volumes are observed and their regional distribution, especially that of the AW, is very patchy. According to this, and to the fact that winter convection reaches to different depth levels annually, a steady development of the physical parameters is not expected in this layer while long term trends may have to be envisaged.

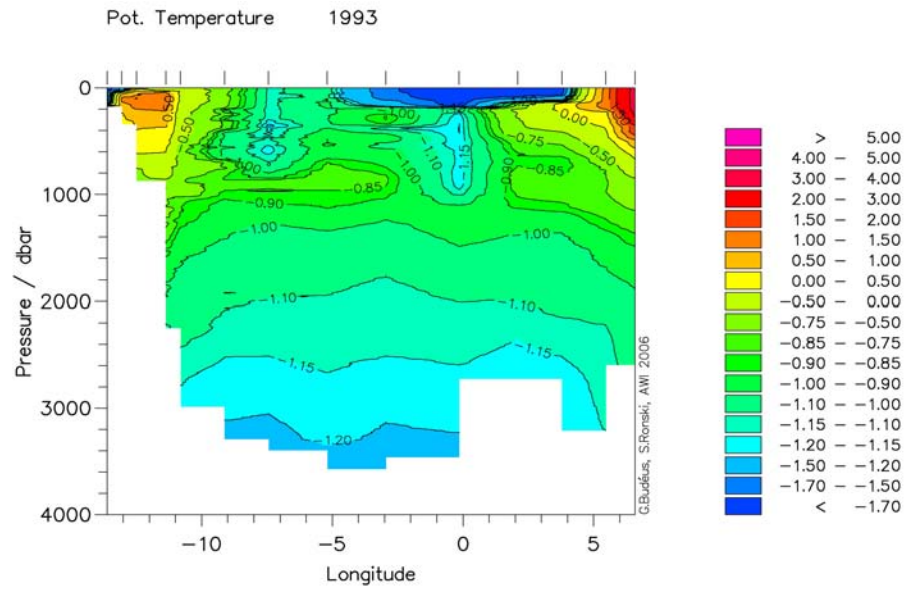
Atlantic Water Influence

Atlantic Waters or their derivatives surround the Greenland Gyre. They are separated from the central gyre's waters by the Arctic Front in the east and an unlabelled subsurface front in the west. In summer, these fronts can be recognised best in the salinity distribution. Indications for an exchange across these fronts have already been identified in the transect plots. Indeed, warm AW import is necessary if the thermal status quo is to be maintained in the central gyre, as the water column there loses heat in the annual average. AWs and their derivatives are the most important heat source to compensate this loss. We will see below that the temporal development of the salinity in the upper layer of the gyre shows periods of salinity increase between periods of decrease. As ice formation is not active during the years of salinity increase, only AWs and their derivatives can act as the relevant source.

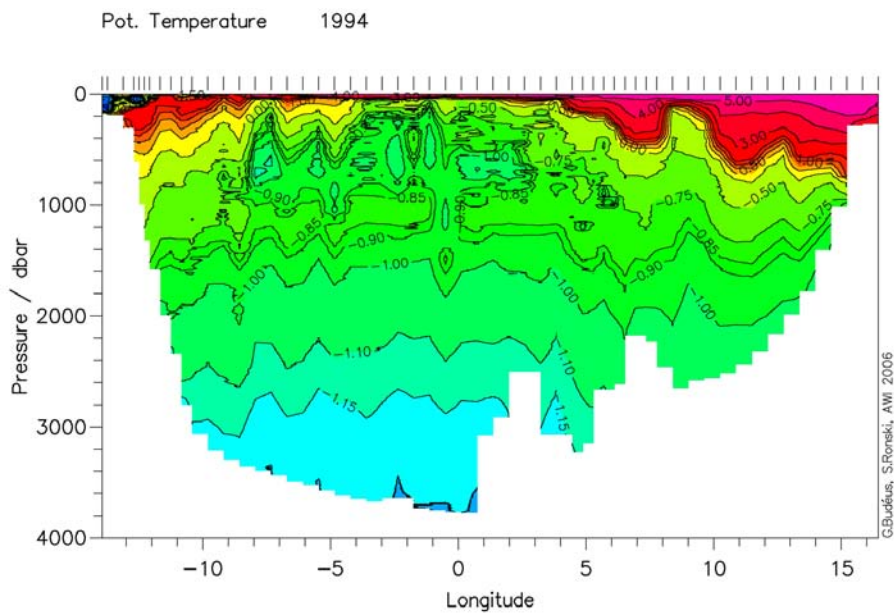
Amazingly, AW patches are absent in most published data sets. Neither the collection of cruises in the 80s presented by [15] nor more recent publications as [21], [22], or [23] show AW in the Greenland Gyre at all. In contrast to this, AW patches in the Greenland Gyre are abundant in our data set during almost every cruise (particularly illustrative examples are 1994, 1999, 2000, 2001, 2002). We suspect that this fact is due to the spatial resolution of the observations, as the general need of an AW import to compensate the mean heat loss to the atmosphere prevails over many decades. Other cruises with a station spacing similar to ours (e.g. [20], their Fig. 22) indeed detect likewise amounts of AW patches.

The fact that AWs are imported by well defined patches stays in contrast to the assumption of a smooth and steady transition from the hydrographic conditions at the rim to those in the gyre's centre. As concepts of deep water formation by double diffusion [24] are developed on the basis of this assumption, they do not seem to be applicable during the 90s.

a)



b)



c)

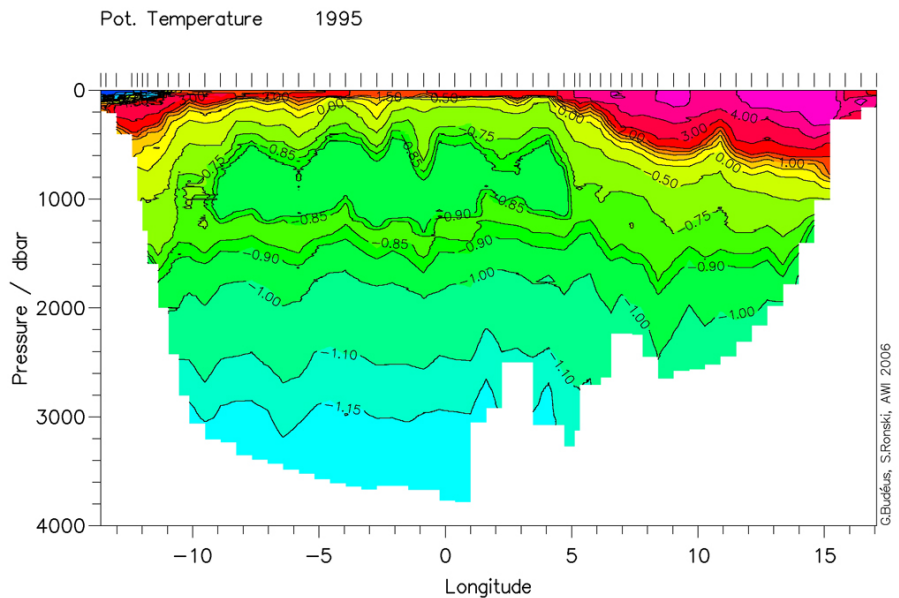
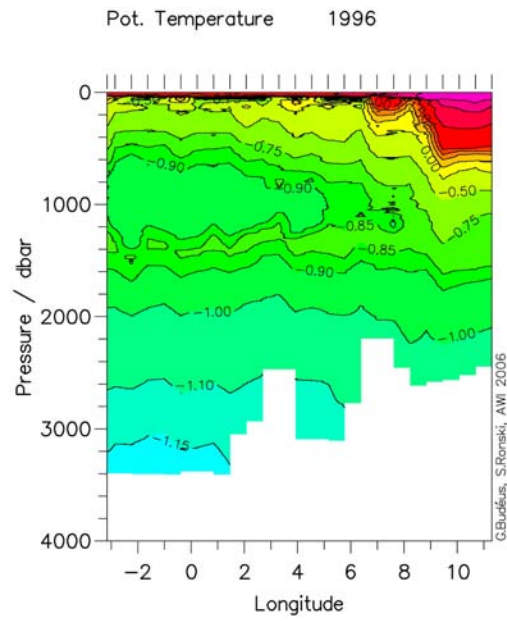
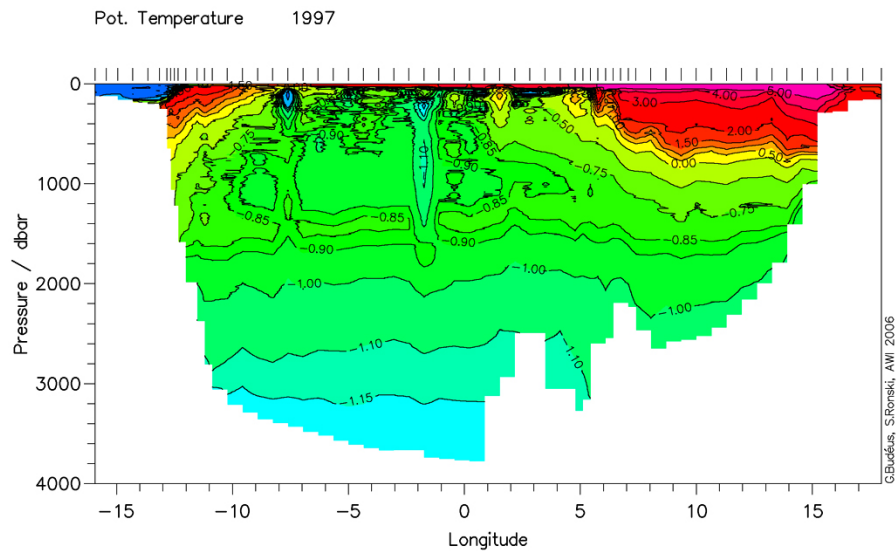


(Fig. 2) contd....

d)



e)



f)

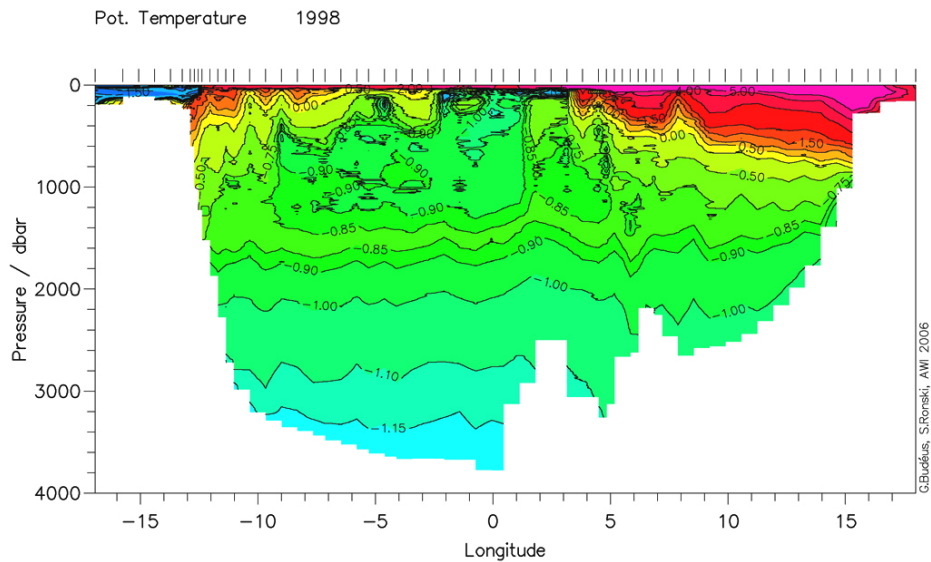
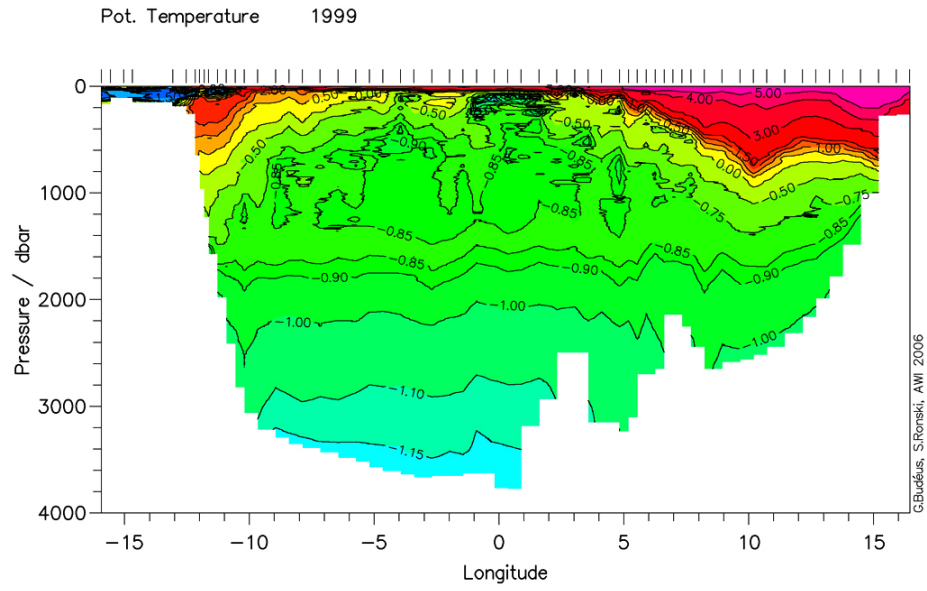
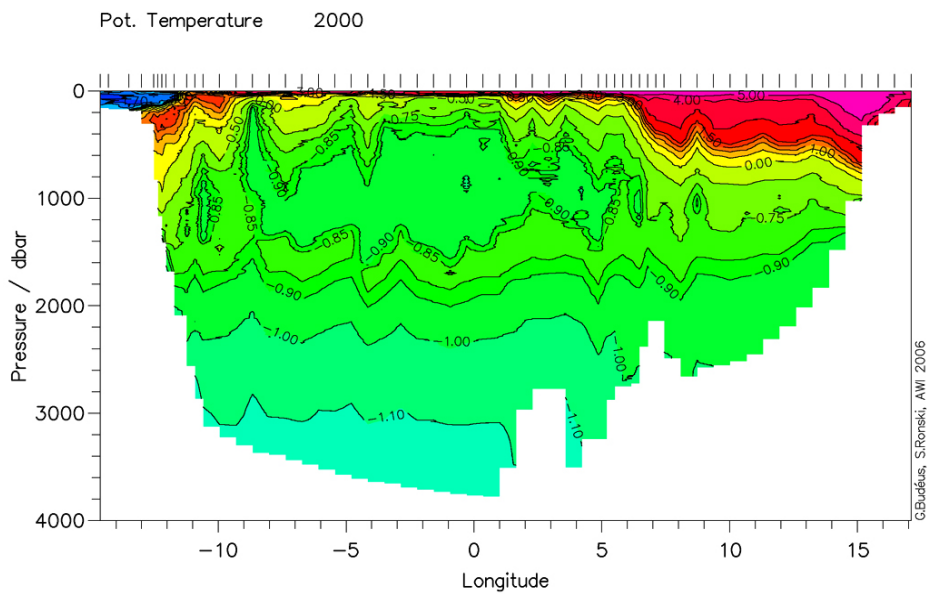


(Fig. 2) contd....

g)



h)



i)

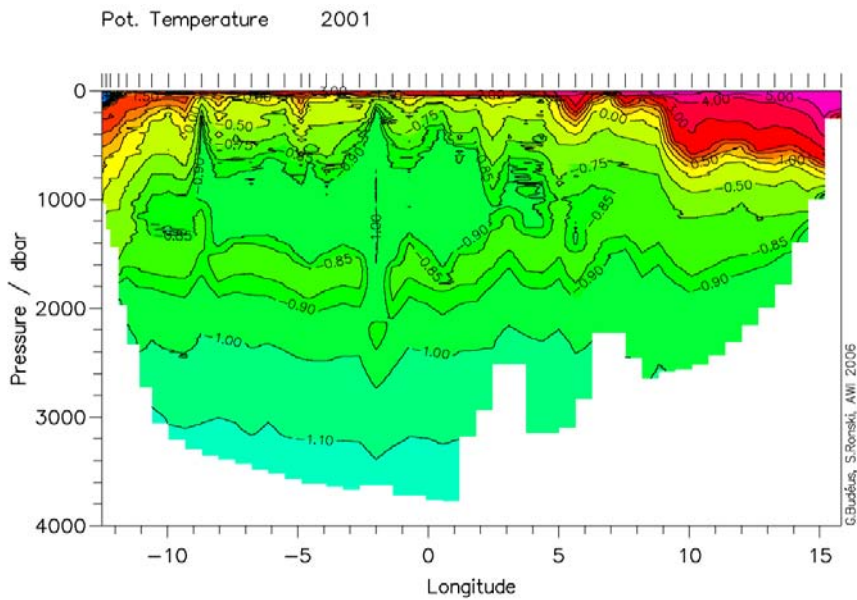
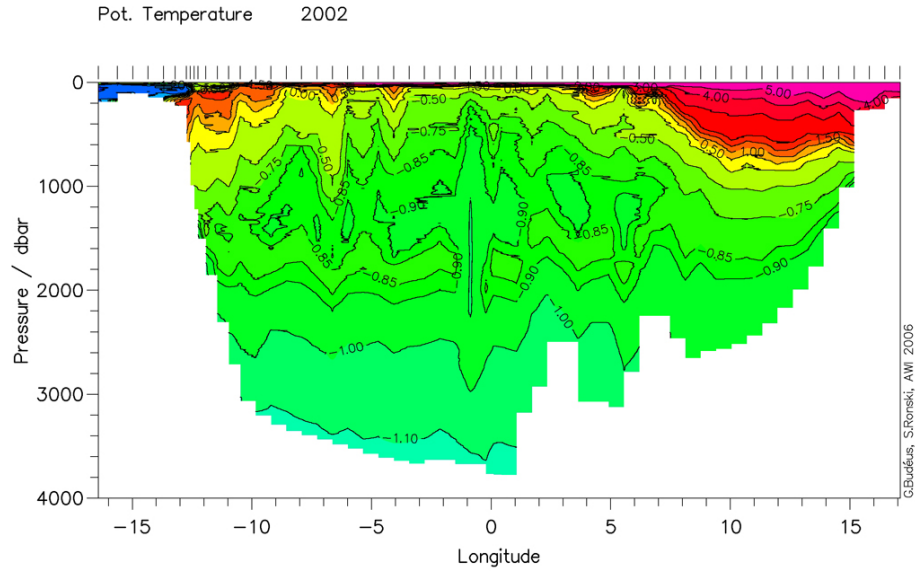
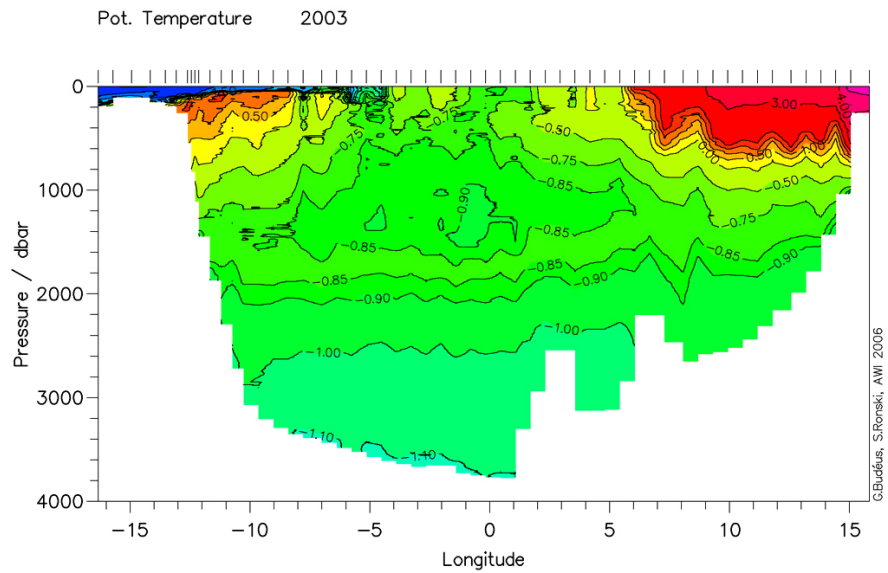


(Fig. 2) contd....

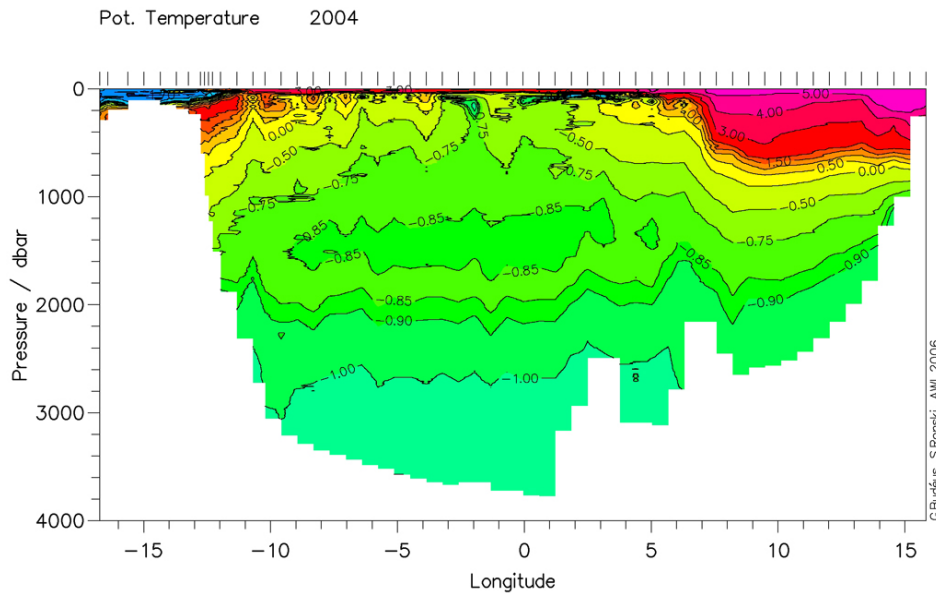
j)



k)



l)



m)

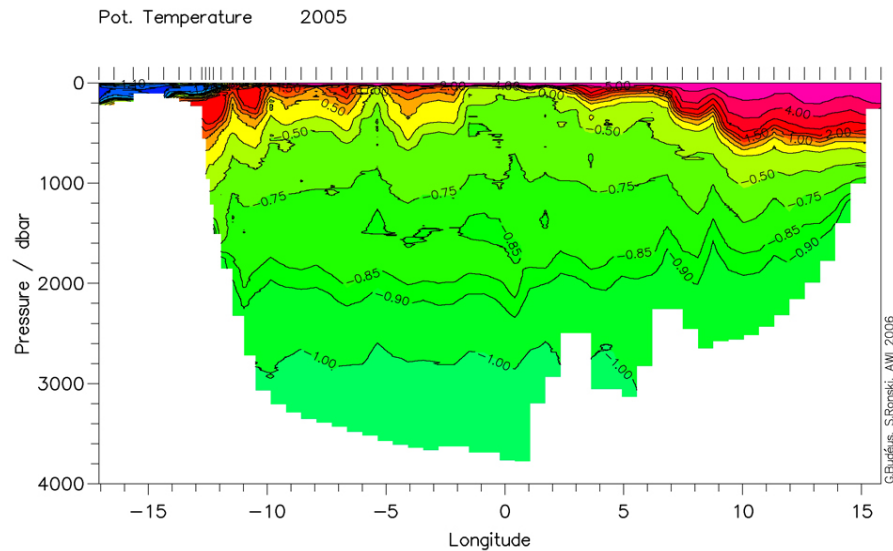


Fig. (2). Pot. temperature distribution at 75°N a) 1993, b) 1994, c) 1995, d) 1996, e) 1997, f) 1998, g) 1999, h) 2000, i) 2001, j) 2002, k) 2003, l) 2004, m) 2005.

The AW patches appear to have diameters of only about 20 km as they are limited mostly to one or two of our stations. Their vertical extent varies from about 200 m as a minimum (see e.g. 1994, 1998) over 300-400 m (e.g. 2000, 2001) to occasionally 1000 m (2002). Thus, the upper few hundred metres are certainly modified continuously in the course of a year by their import. The AW import will partly be compensated by an export at the same levels. Such an export of the Greenland Sea upper layer waters across the fronts has direct implications for the modification of the water masses within the great rim current systems passing the gyre. The export contains a mixture of AW and PW which is also imported: the PWs are first imported into the Greenland gyre, are vertically distributed and mixed with AW by convection, and are redispensed into the Atlantic Water domains thereafter. This establishes an indirect way to freshen the EGC core by an admixture of PW.

AW has long been regarded as adverse to winter convection according to its large heat content. An analysis of winter convection during our time series shows that this perception is not correct and that the AWs act as an efficient salt source which enables winter convection during numerous years [25]. The ratio between AW and PW determines greatly the temporal evolution of temperature and salinity (and convection history) in the upper layer, and both imports will provide a contribution to the volume increase of the upper layer which is related to the descent of the interface.

Convection

Evidently, it is most important to determine convection depths correctly, because convection stays in interplay with advective processes and erases the advective signal with its associated modifications. Thus, observed modifications in the entire upper layer can be attributed to a related process only after convection depths are defined properly.

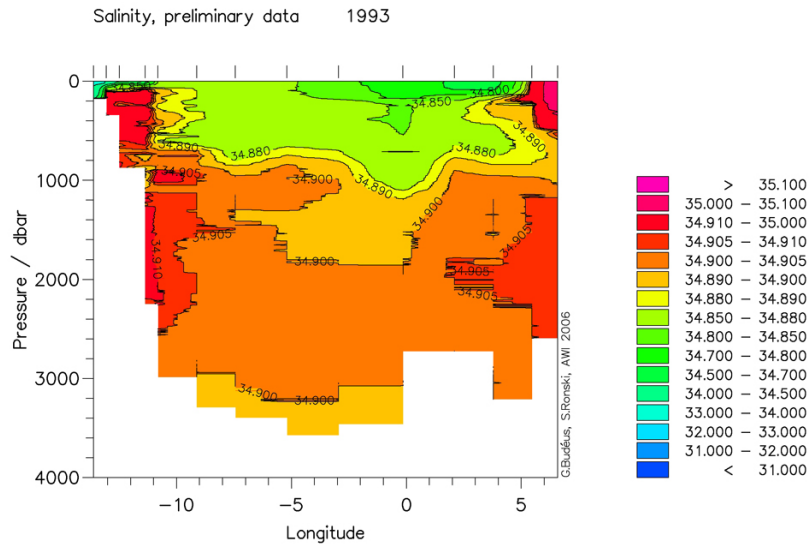
In the Greenland gyre, transformation of surface waters into intermediate waters is forced by air-sea interaction. Various factors are commonly discussed which are supposed

to control convection depth. These are the magnitude of heat loss (note that annual averages need to be winter centred to be applicable for this purpose), the surface salinity or surface fresh water content (with high fresh water contents being adverse to winter convection), the local ice formation (with its associated brine release), the previous ventilation history, and the actual vertical structure of the water column.

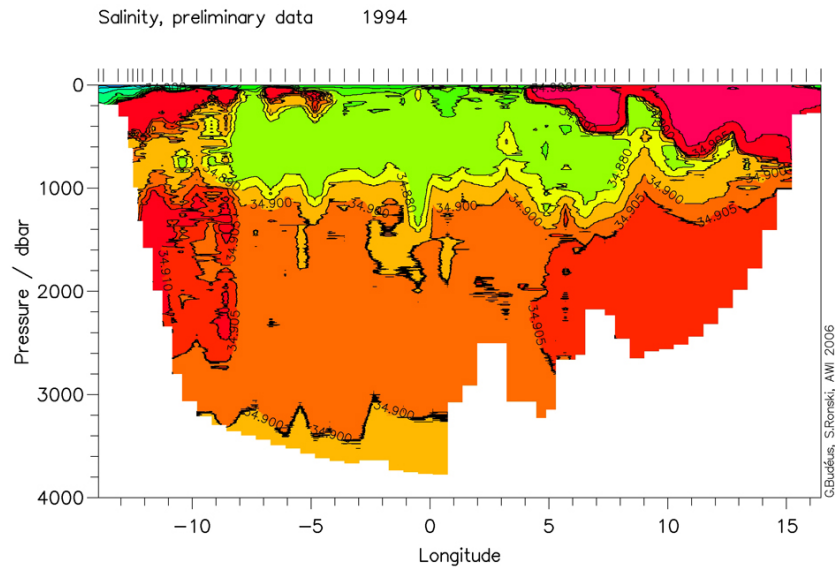
It has been shown for the Greenland Sea that higher heat losses are not synonymous with deeper convection depths and that the occurrence of ice formation is not a good indicator for particularly strong convection [25,26]. Though evidently initially forced by the heat loss to the atmosphere, the convection depth and the affected volume are controlled mainly by the structure of the water column which is present before the convection phase. A detailed discussion about the relative importance of the magnitude of heat loss, ice formation, strength of the fresher surface layer and their relation to observed convection depth is found in these publications and we only refer to the determination of convection depths here.

Advective modification works in the entire upper layer, so that after the 'reset' by winter convection, continuous changes are expected in the course of the other seasons (and each winter's individual convection depth defines the downward limit of 'seasonality' for the respective year). Despite the ongoing advective modifications, convection in the Greenland Sea can be detected by comparison between two successive years because the direction of modifications by advection is well defined: Advection always introduces a tendency to higher salinities, higher temperatures, lower densities and higher stabilities according to the differences between the gyre centre with its 'cold lens' and the warmer and saltier rims. If, on the other hand, a temperature reduction, salinity reduction, density increase or homogenization (stability reduction) is observed in comparison to the previous year, they can only be caused by winter convection and serve as positive criteria for winter convection. It is important to note that in contrast to general assumptions convection in the Greenland Sea can result in a temperature and

a)



b)



c)

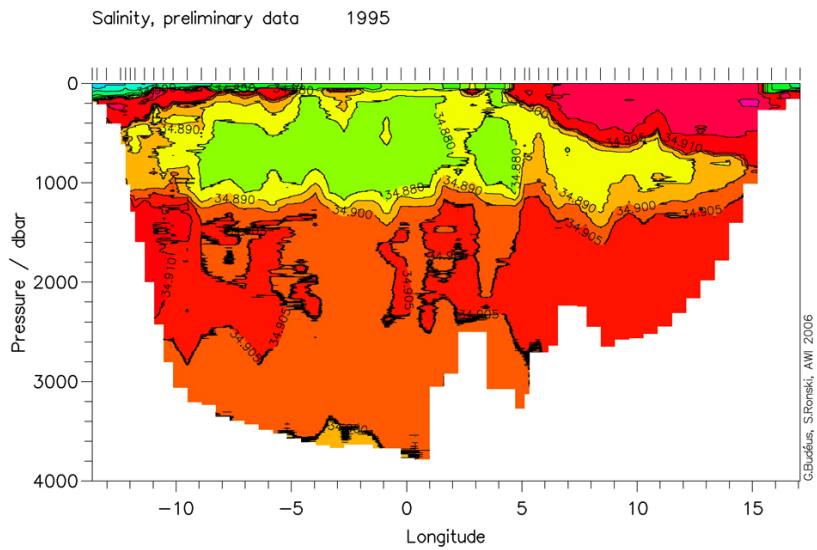
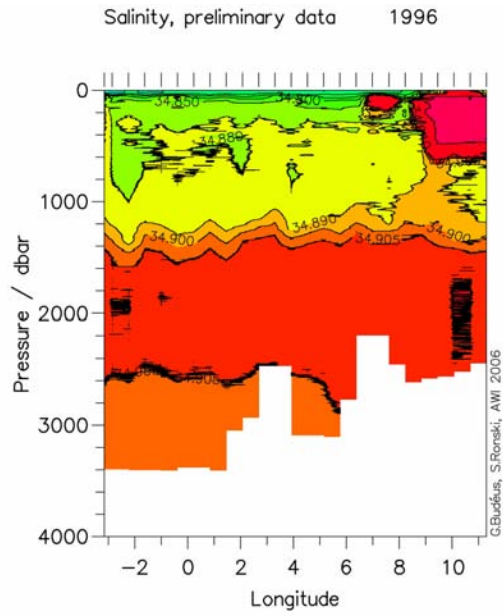
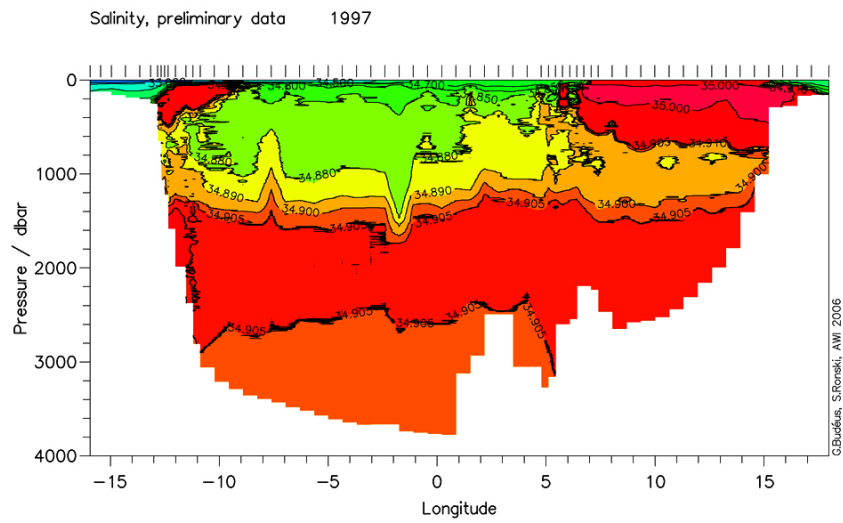


(Fig. 3) contd....

d)



e)



f)

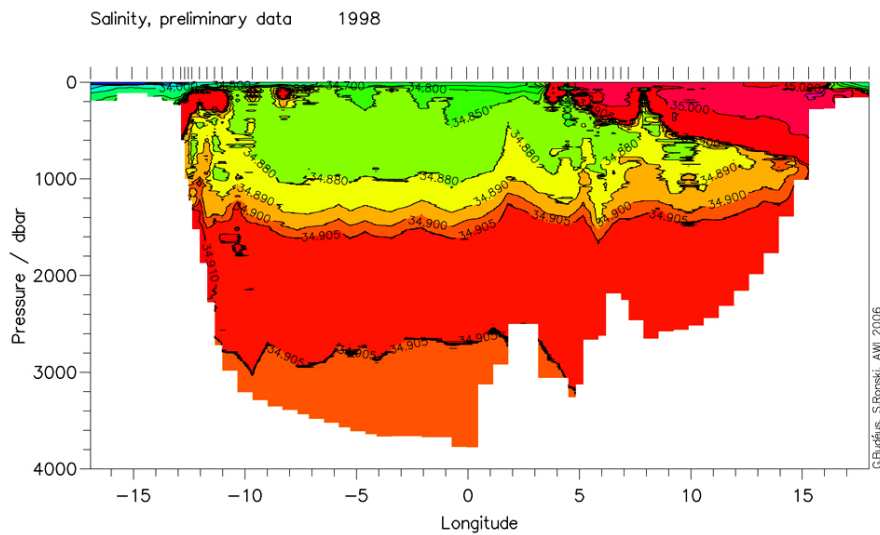
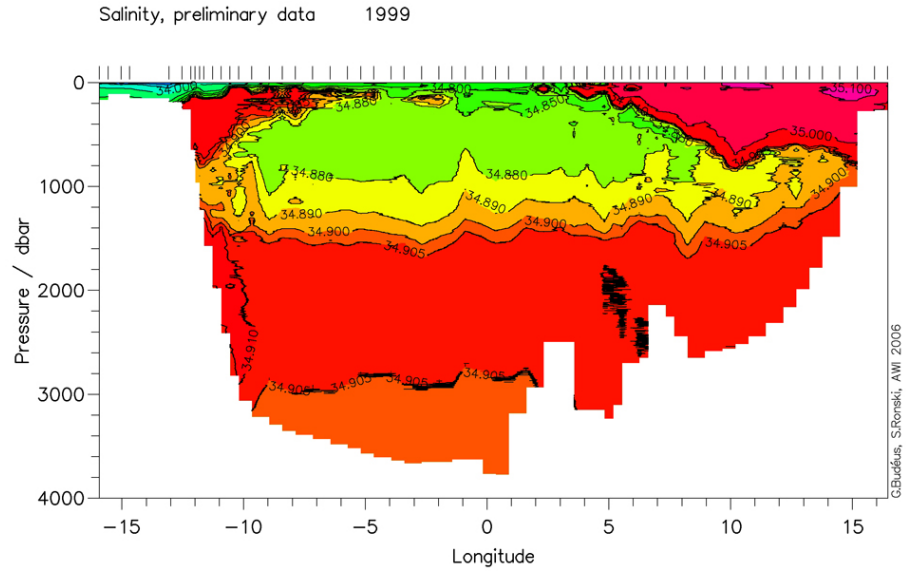
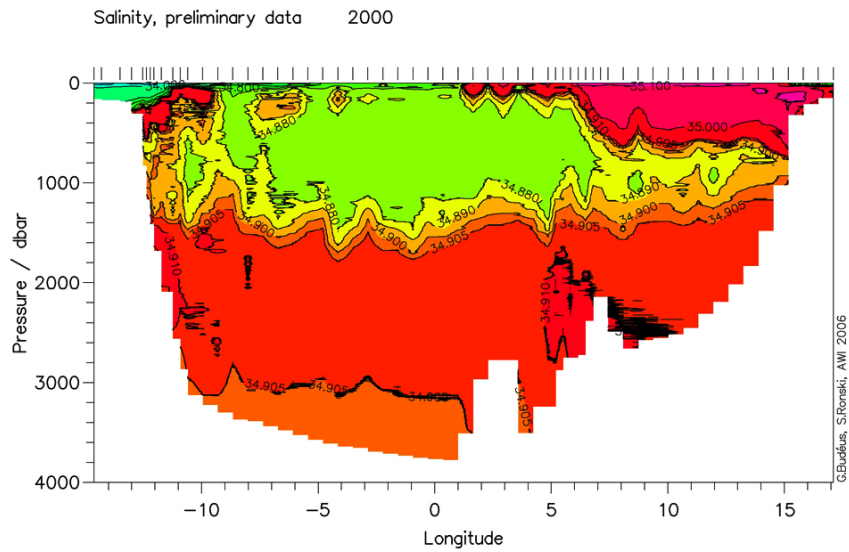


(Fig. 3) contd....

g)



h)



i)

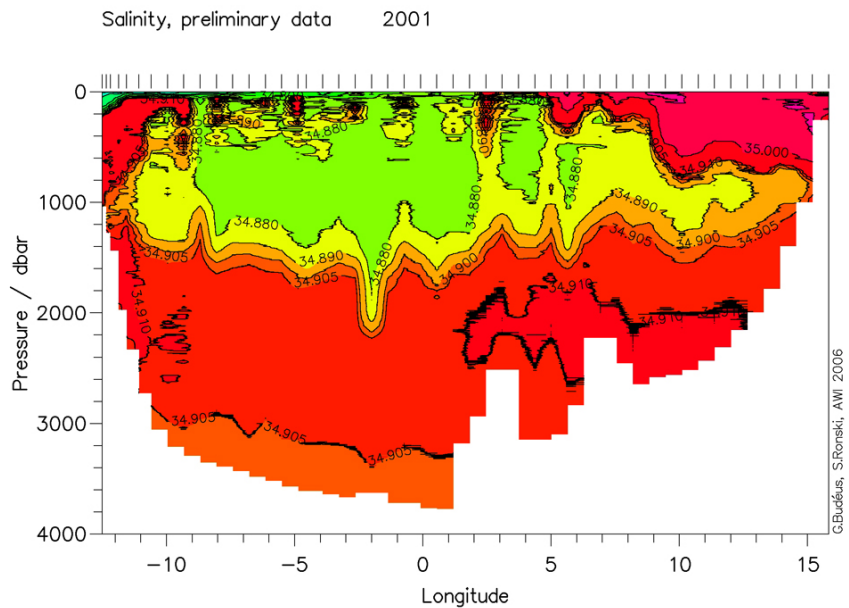
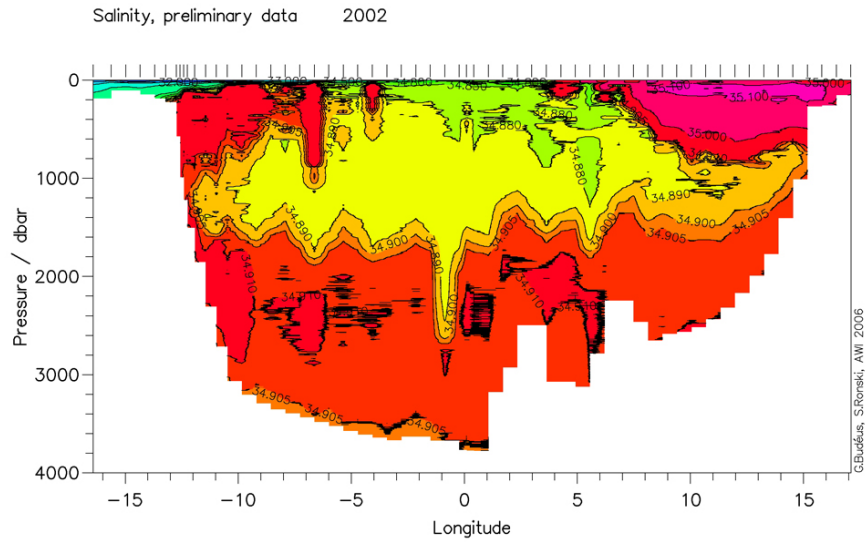
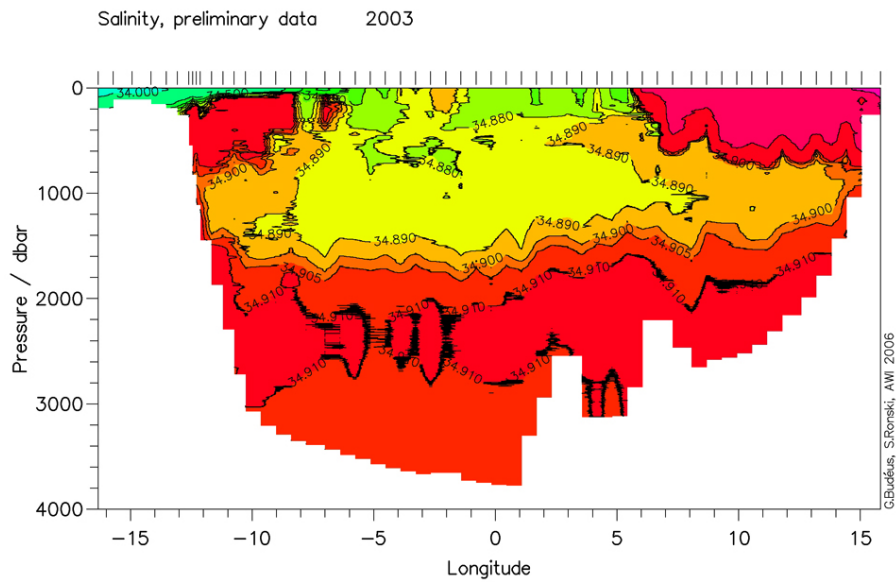


(Fig. 3) contd....

j)



k)



l)

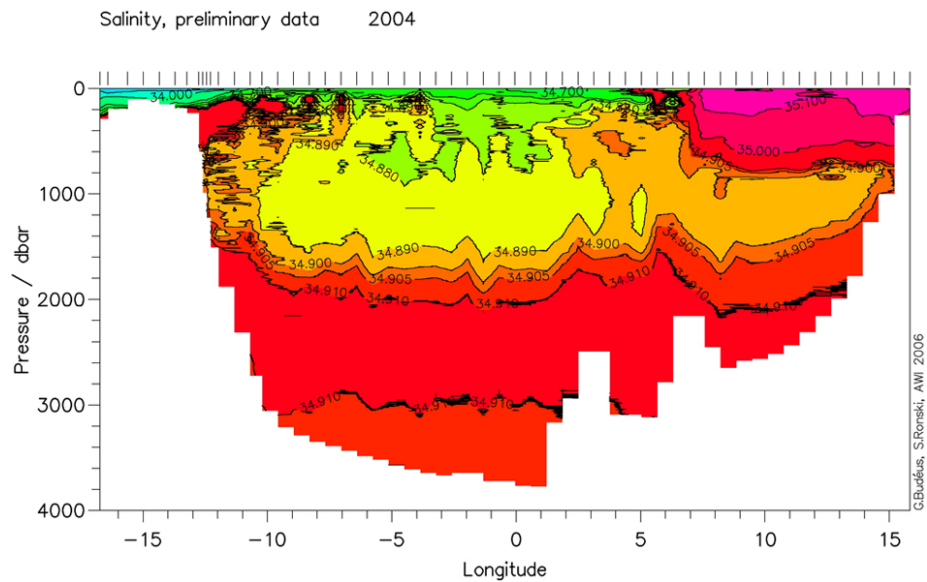


(Fig. 3) contd....

m)

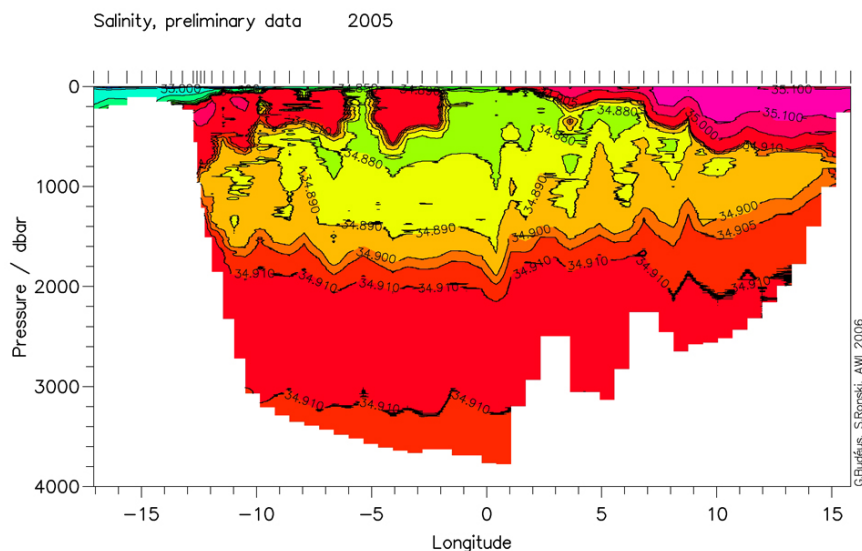


Fig. (3). Salinity distribution at 75°N a) 1993, b) 1994, c) 1995, d) 1996, e) 1997, f) 1998, g) 1999, h) 2000, i) 2001, j) 2002, k) 2003, l) 2004, m) 2005.

salinity increase, and also stability can be maintained after convection events. This means that the absence of cooling can by no means be taken as an indicator for the absence of convection, as is often implied in the literature. On the other hand, if only one of the positive criteria mentioned above is met, convection is unambiguously identified.

A criteria catalogue for convection depths is developed and discussed in detail by [26] and the time series of convection depth, as analysed from these criteria, is shown in fig. 6. This history of convection depths is obviously not in accord with other recent publications. [22] propose a deep convection event for winter 1996/97, and [23] identify only two convection events (1994/95 and 1999/2000) during the discussed period. For the first - convection to deep sea levels - we find no indication in our data set. The deep temperature structure remains unchanged between 1996 and 1997, and the intermediate temperature maximum is not destroyed. We recognise no cooling in the deep waters: The mean profiles in the gyre centre (Fig. 7) show cooling to a depth of about 600 m, which is accompanied by considerable freshening. Although the individual profiles of the data set are not shown by [22], we guess that a profile in a CV or nearby is contained in the 1996 data, resulting in exceptional warm temperatures below the interface at this site (compare CV occurrences in the transects and see the CV chapter). This assumption is corroborated by the fact that the deep water temperature dip in the time series is not apparent in [23] who use the same data set but screen for and exclude CVs.

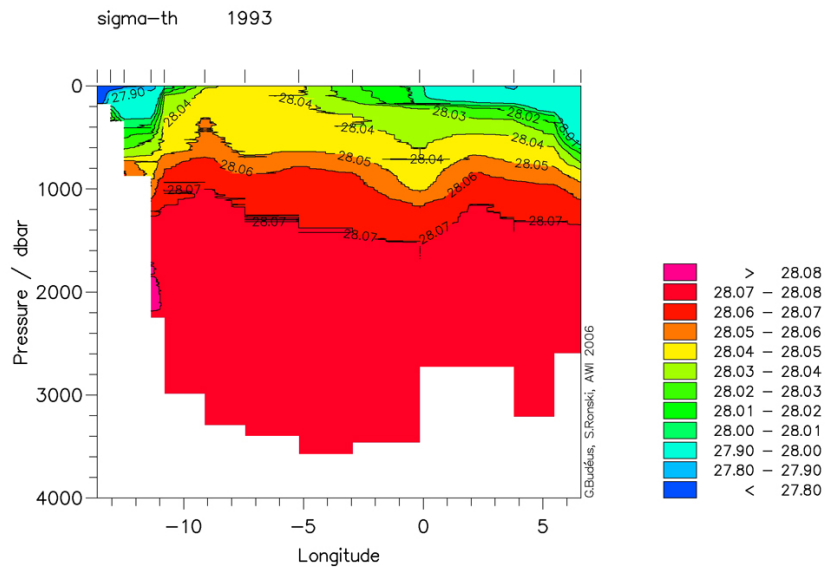
With respect to the second publication, there is a striking contrast between the regular winter convection determined by us and the only two convection events identified there. It seems as if the CFC inventory is not a suitable indicator for convection under the conditions present in the Greenland Sea. Indeed, the descent of the interface causes a corresponding increase of the upper layer's total volume, and if this is filled by import close to the surface (as we suggest), the CFC inventory change is substantially dependent on the import rate and interface descent.

Temperature and Salinity Development

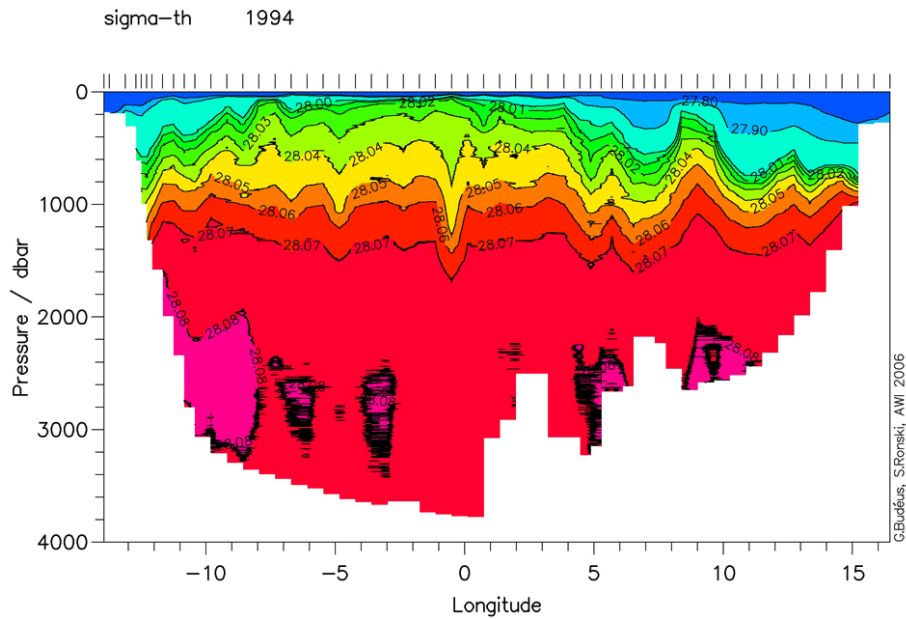
Both salinity and temperature developments in the upper layer are dominated by the interplay between convection and advective modifications. As slow advective modification follows after the rapid changes introduced by winter convection, it is impossible to define an approximate maximum level down to which 'seasonality' affects the actual hydrographic conditions: Each year's individual maximum convection depth defines this level anew. Atmospheric heat input during summer also plays a role, but is likely to be confined close to the surface, due to the highly stratified summer conditions. For the subsurface levels, the advective signal of the AW import plays certainly a more prominent role than atmospheric heat input.

The important influence of the AW input can immediately be seen in the salinity development (Fig. 8). In the upper layer, several periods of salinity increase (1994-1996, 1998-2002) stand out between periods of freshening. The relevant salt source are the AW derivatives which outweigh the contributions of PW during these years. When AW are distributed vertically by winter convection, the salinity increase can occasionally be recognised to depths just above the salinity/density step. A mixed layer type ventilation is related to this [26]. In contrast, plume convection transfers fresher waters to greater depths and is effective when the PW input dominates. As both ventilation types alternate, periods of freshening alternate with periods of salinification. There is no unilateral trend in the upper layer's salinity, and depending on the starting point, trends over only a few years might show either direction. The development of the mean salinities in the layer between 10 and 200 m (Fig. 9) shows that an overall freshening trend, as discussed in climatic contexts, is not apparent during our investigation period. Fresh water pulses appear in 1996 and 2004, but disappear again later. The 1996 pulse is presumably related to an increased southward fresh water transport by the EGC through Fram Strait which is identified in simulations by [27].

a)



b)



c)

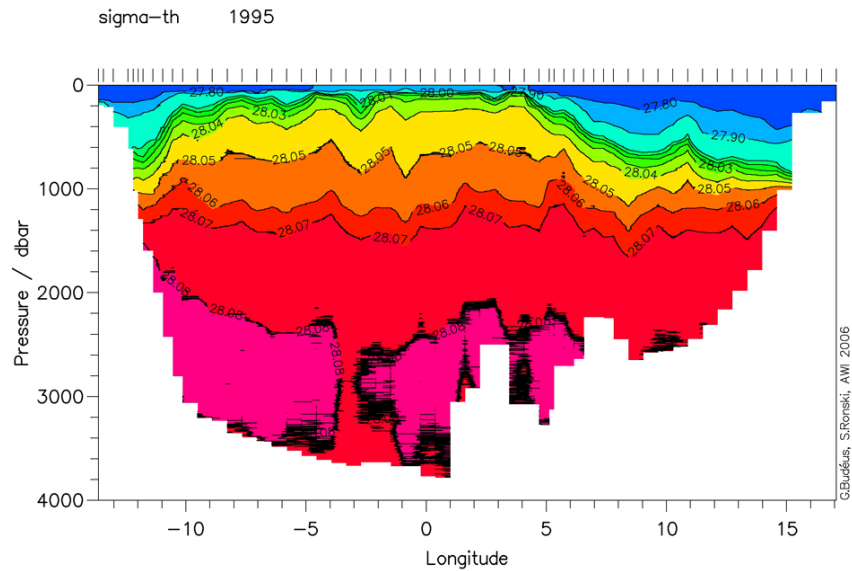
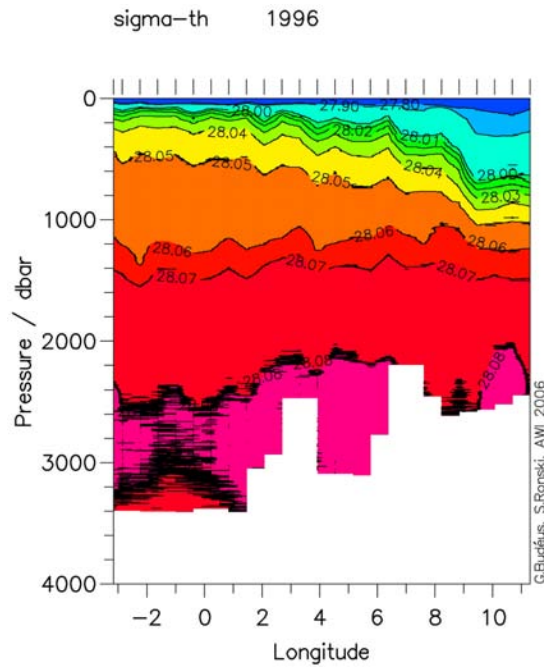
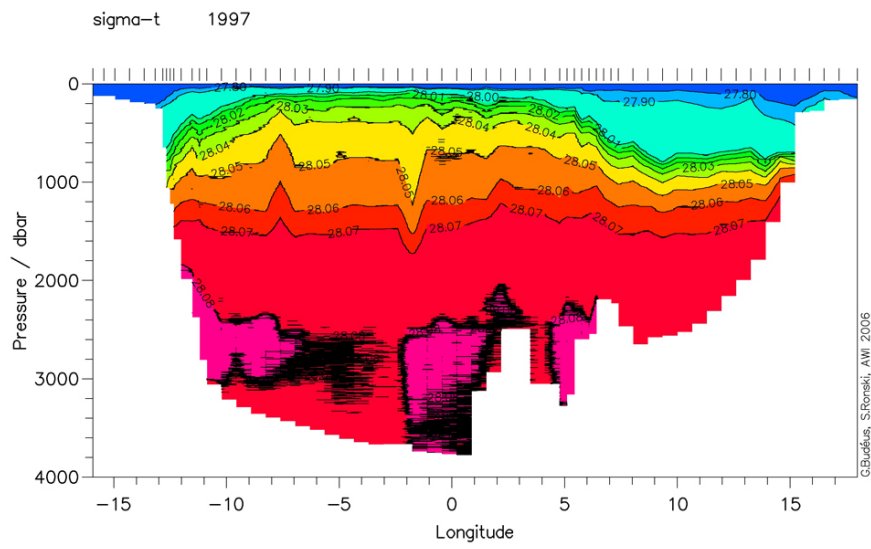


(Fig. 4) contd....

d)



e)



f)

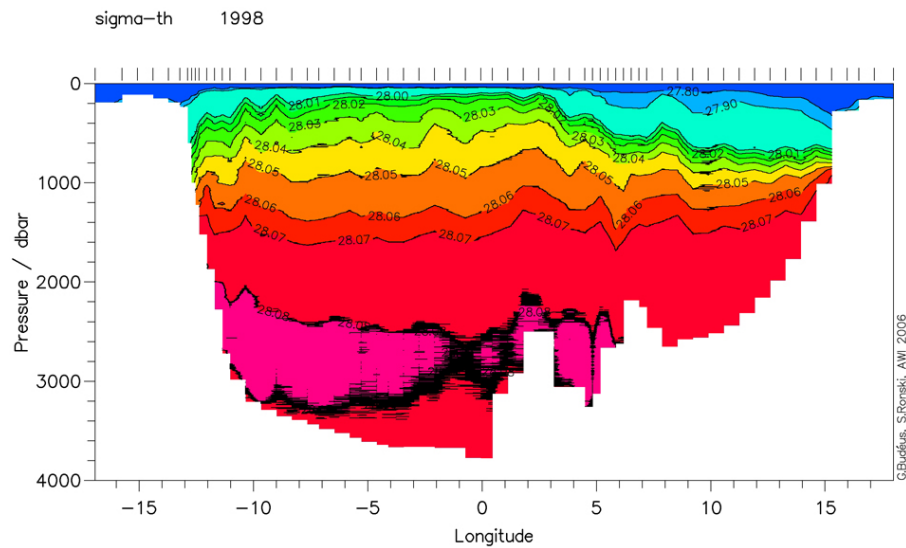
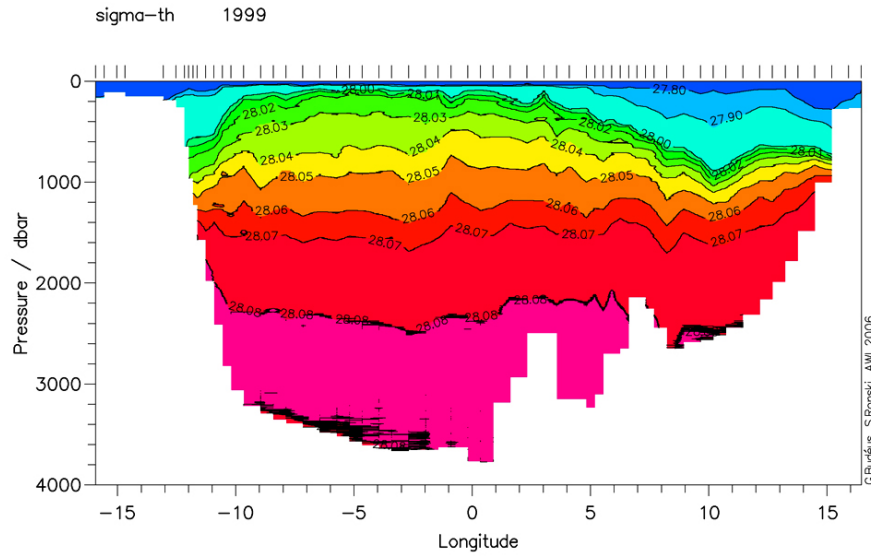
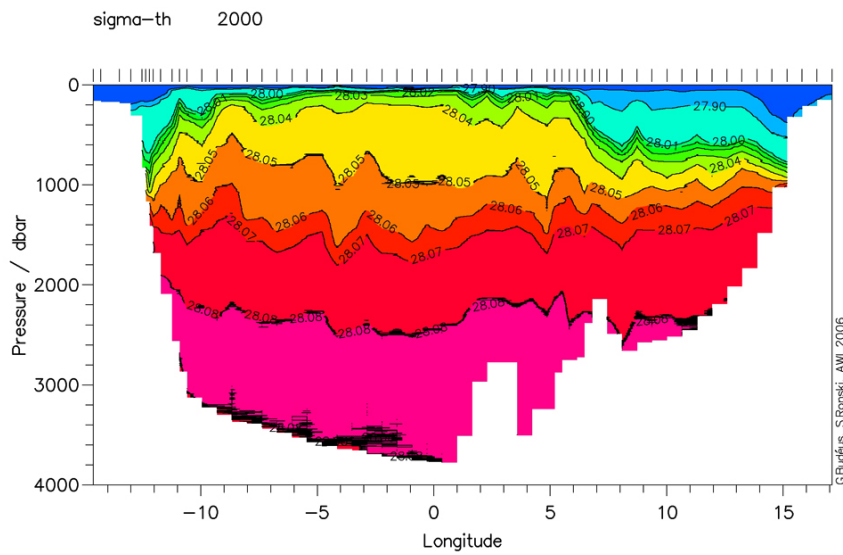


(Fig. 4) contd....

g)



h)



i)

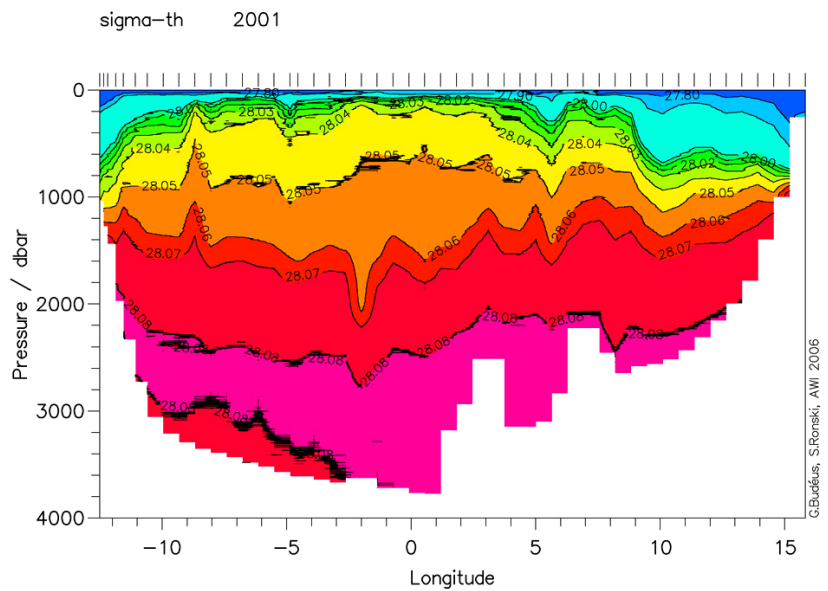
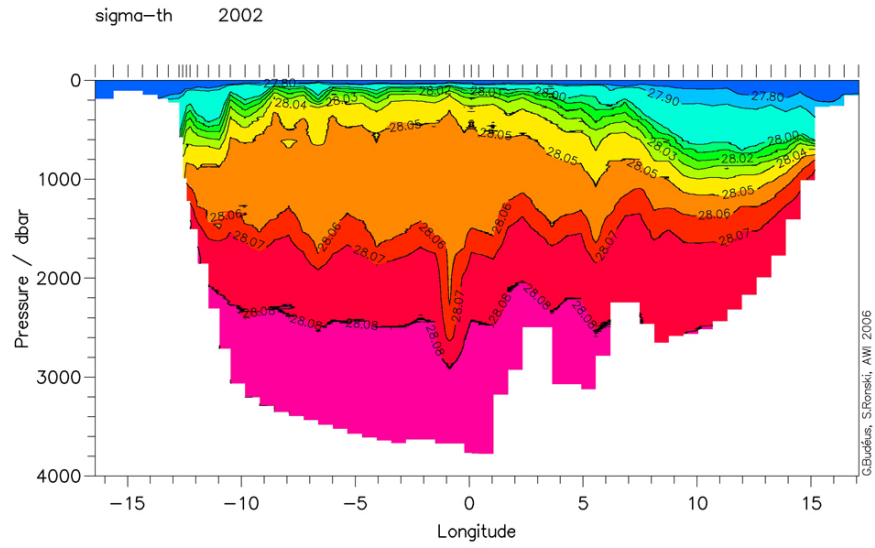
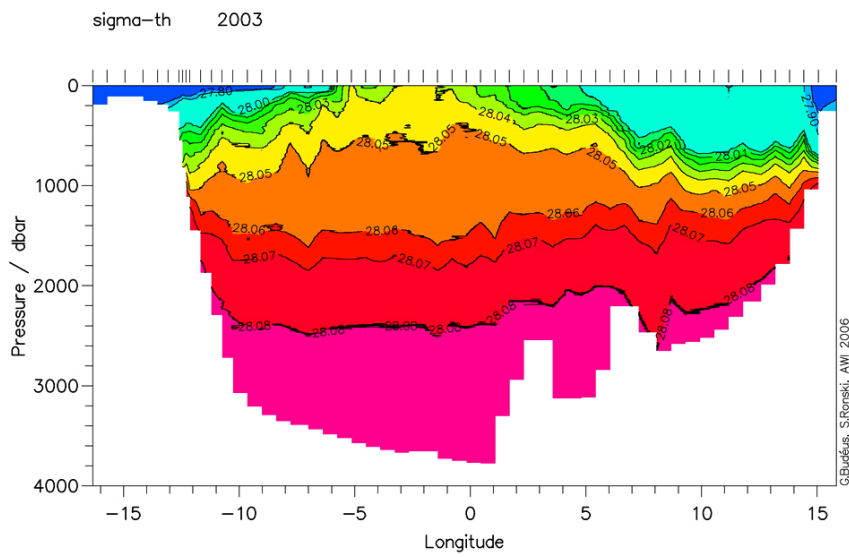


(Fig. 4) contd....

j)



k)



l)

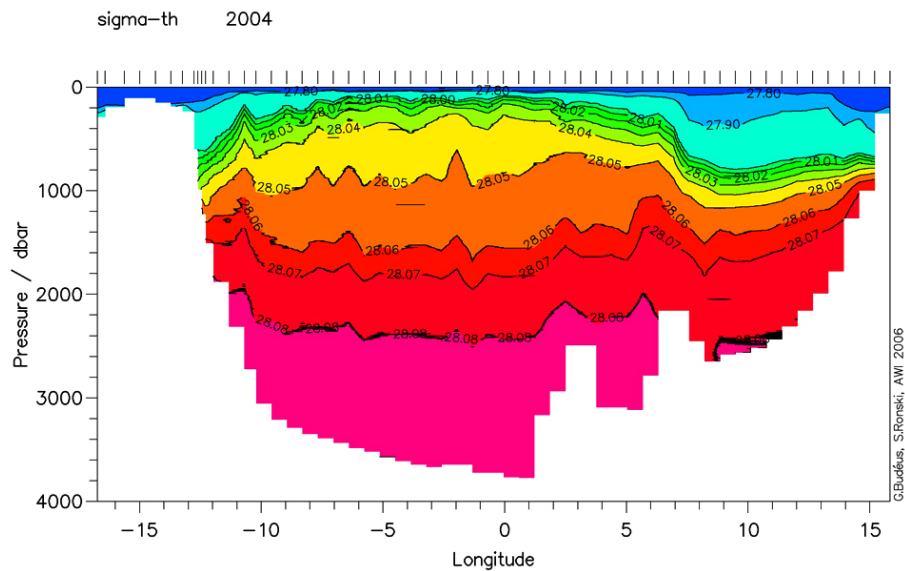


(Fig. 4) contd....

m)

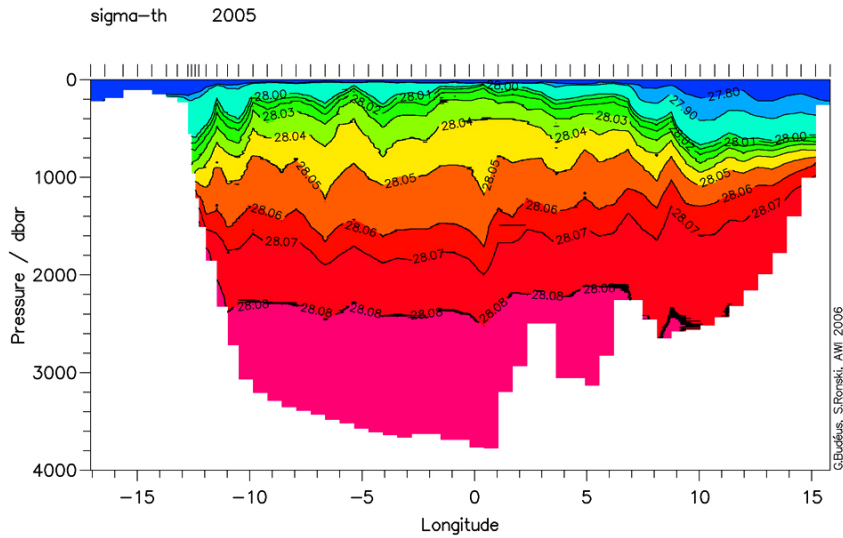
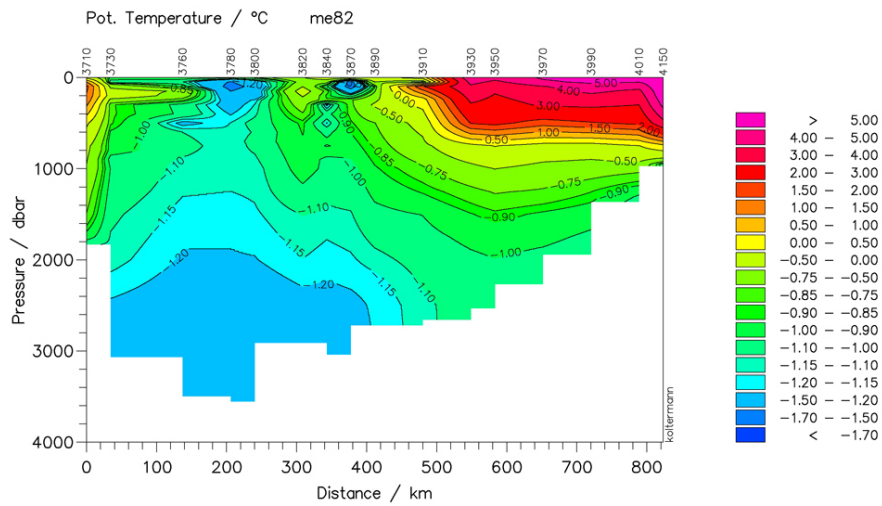


Fig. (4). Potential density distribution at 75°N a) 1993, b) 1994, c) 1995, d) 1996, e) 1997, f) 1998, g) 1999, h) 2000, i) 2001, j) 2002, k) 2003, l) 2004, m) 2005.

a)



b)

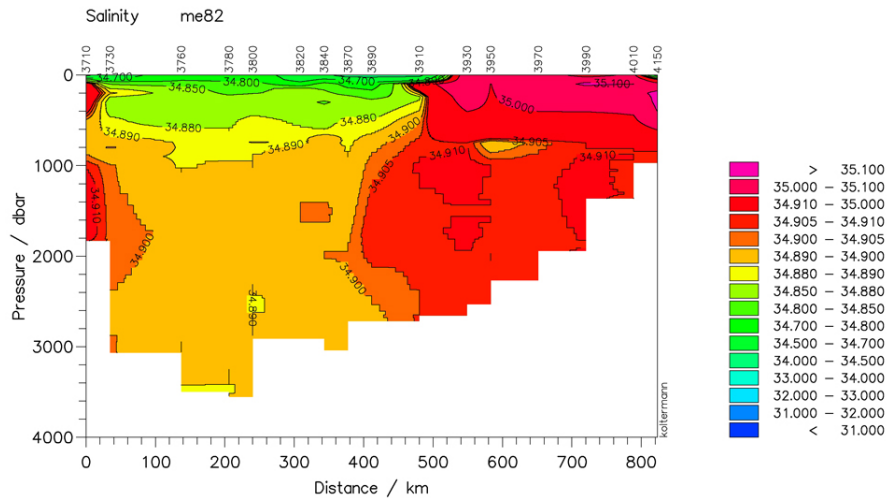


Fig. (5). a) Temperature and b) Salinity distribution on NW to SE transect, 1982, replotted from the data set published by [15], and available from DOD.

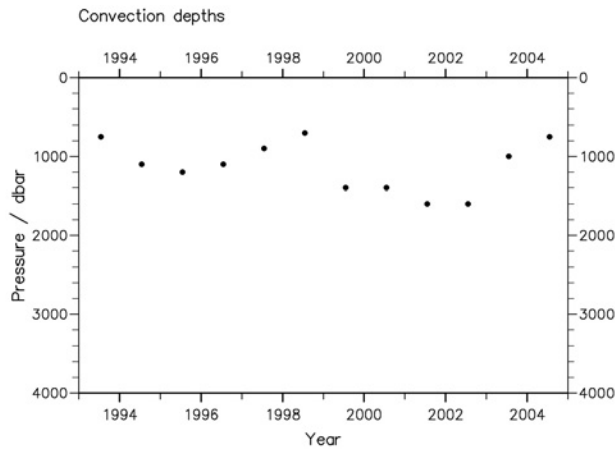


Fig. (6). Convection depths as analysed according to a multi-parameter catalogue.

The absence of a steady trend is similarly true for the temperature development (Fig. 6), where periods of cooling and warming alternate. While cooling is unequivocally attributed to winter convection, warming below the summer surface layer might be caused by exchange with the rims or by winter convection with a large AW contribution. It can be shown that the latter is indeed the case e.g. for the warming trend from 2000-2001, or also from 2001 to 2002: The warming of considerably deep waters (within the here discussed upper layer) by winter convection is documented by winter measurements of an autonomously profiling CTD-mooring (EP/CC-Jojo, [28]). When winter convection does not extend to the salinity/density step, a steady temperature increase is always observed between the maximum convection depth and this step. This observation indicates that advective processes modify in principal the entire upper layer, though at a slow pace in its deeper parts.

Density and Stability Development

The generally weak stratification in the region in combination with the variations of seawater compressibility due to

temperature differences renders comparisons of potential densities referenced to any fixed pressure level almost useless for the determination of interannual density changes. Therefore we show in Fig. (10a) the anomaly of insitu densities relative to an initial profile in 1993. The overall perception of the density and stability changes is hindered by the descent of the interface with its enhanced salinity and density gradients. Above the interface, densities are markedly smaller than below and so any movement of the interface dominates the plot of the density and stability development.

The large and steady density decrease between 1000 and 2000 dbar is this signal of the descending interface; it is not due to a modification within the moving interface itself (see chapter 'Interface'). Above about 1000 dbar, temporal variations are due to modifications of the upper layer water pool. Interannual changes are prominent above this level. It seems as if we start with a relatively dense state in 1993, but this is an arbitrary initial state and we want to focus on the relative changes here. A period of densification is seen at the beginning of the time series (1994 to 1996, $\Delta\sigma_{1994to1996} = 5 \text{ g/m}^3$), followed by a development to lighter waters (1996 to 1999, $\Delta\sigma_{1996to1999} = -10 \text{ g/m}^3$) and a second densification period (1999 to 2000, $\Delta\sigma_{1999to2000} = 7.5 \text{ g/m}^3$). Less pronounced variations prevail between 2000 and 2003 with $\Delta\sigma$ excursions to ± 0 and $+3 \text{ g/m}^3$ (relative to 1993). A tendency to smaller density follows between 2003 and 2005 ($\Delta\sigma_{2003to2005} = -12 \text{ g/m}^3$).

As the only source for a density increase is winter convection, convection is readily identified for the respective years. But also during most other years, we identify convection to considerable depths. This means that the interplay between advective processes, which lead to a density decrease, and winter convection is such that the former outweighs the latter during those years. A general trend to higher or lower in situ densities in the upper layer of the Greenland Sea is not apparent in the presented time series. Density variations in the range of up to 15 g/m^3 seem to occur frequently and do not establish an irreversible trend.

Similar to the density development, the visual appearance of the stability development (10b) is dominated by the verti-

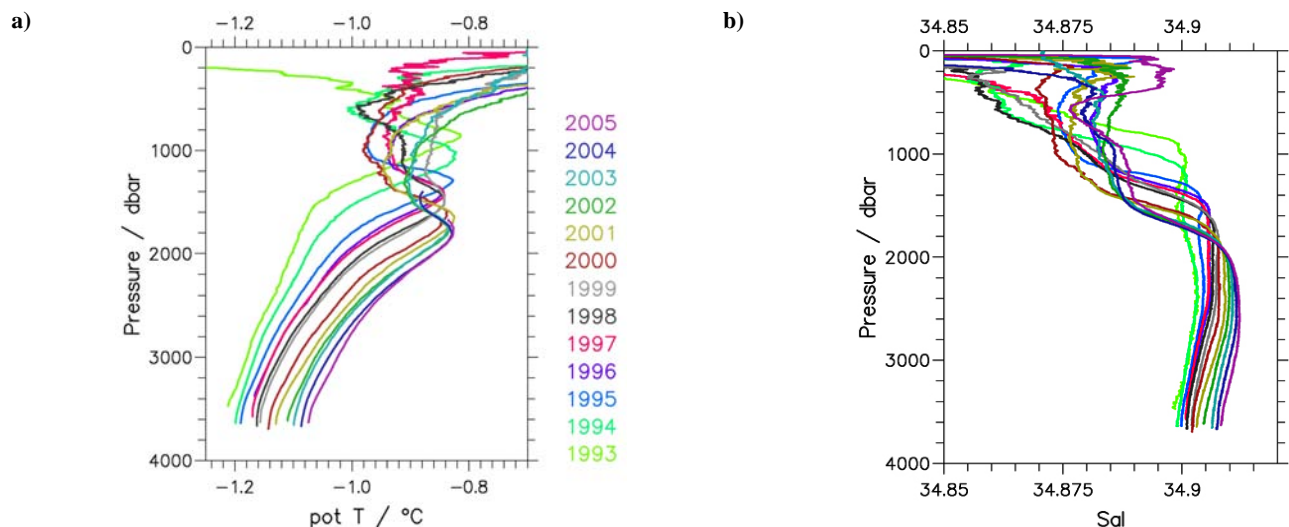


Fig. (7). Mean profiles of a) potential temperature and b) salinity in the Greenland gyre centre. Note that temperature profiles of 2004 and 2005 are truncated shortly above the intermediate temperature maximum to retain an intelligible plot.

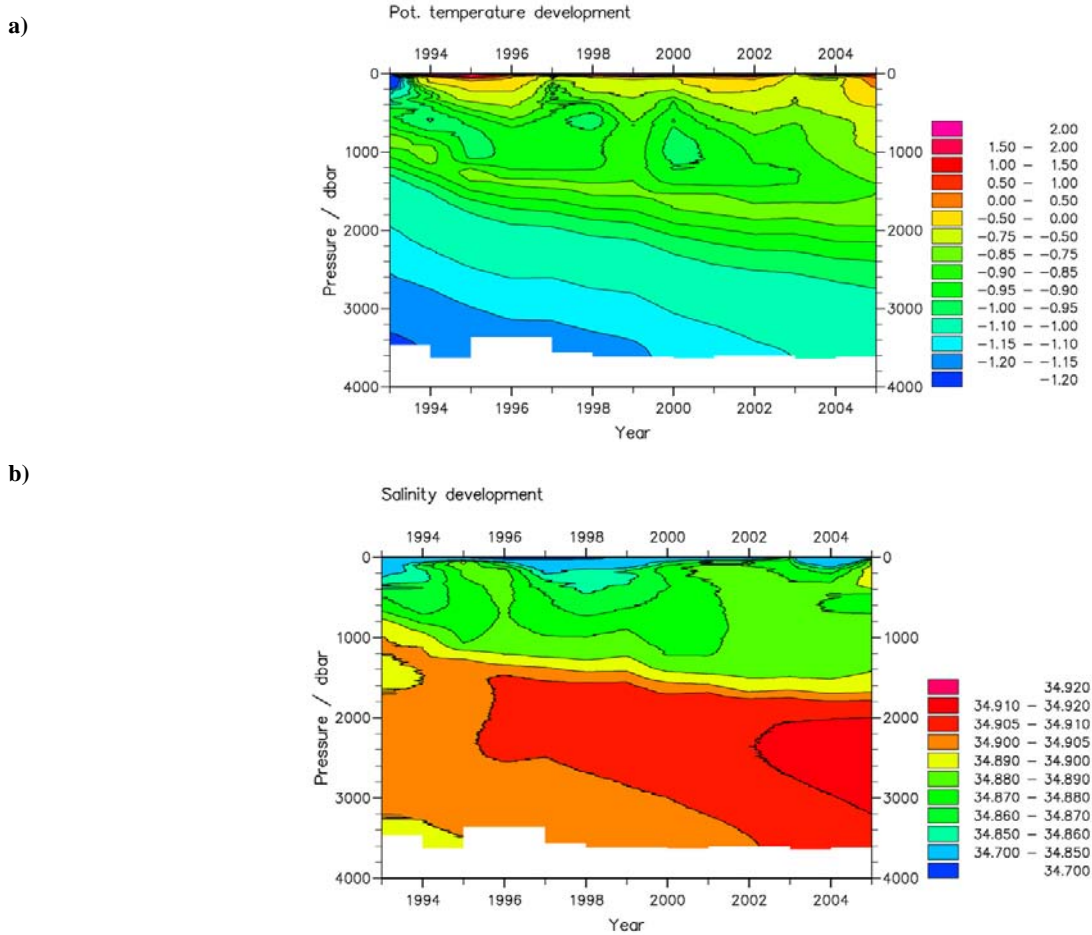


Fig. (8). Development of a) pot. Temperature and b) salinity in the gyre centre.

cal displacement of the interface. The interface is marked by a stability maximum who's magnitude varies only little with time. In contrast to this, the stability development above the

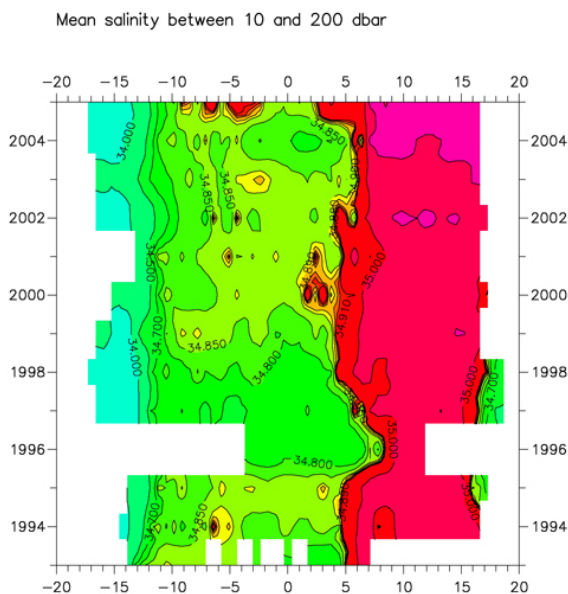


Fig. (9). Development of the mean salinity in the layer between 10 and 200 m from 1993 to 2005 over the entire zonal transect between 20°W and 20°E.

interface shows periods of increasing and decreasing stratification. This is related to the type of convection in winter and its interplay with advection from the rim. Advection into the Greenland gyre leads to a stability increase in the upper layer, and only winter convection can reduce it at depths below the wind mixed layer. However, convection is not always combined with a stability reduction. While a mixed-layer type of convection results in outstandingly homogeneous vertical conditions in the Greenland Sea (as possibly not observed elsewhere), the second type, namely plume convection, does not destroy the vertical stratification [26]. The thermobaric effect is important for the latter convection type and it might therefore be particularly effective in the Greenland Sea.

The developments from 1999 to 2000 and 2000 to 2001 are examples for the homogenisation by the mixed-layer type of winter convection. Note that after the convection phase, stratification will reappear in the course of the year so that the apparent steady stability decrease from 1999 to 2001 will in reality be interrupted by a period of increasing stabilities between spring and the start of winter. The development from 1996 to 1997 is an example for the plume convection type, in this case reaching to about 1100 m. We see that despite this comparatively deep convection, the stratification is not destroyed. Naturally, such a statement cannot be based solely on the shown time series, as there could also occur a

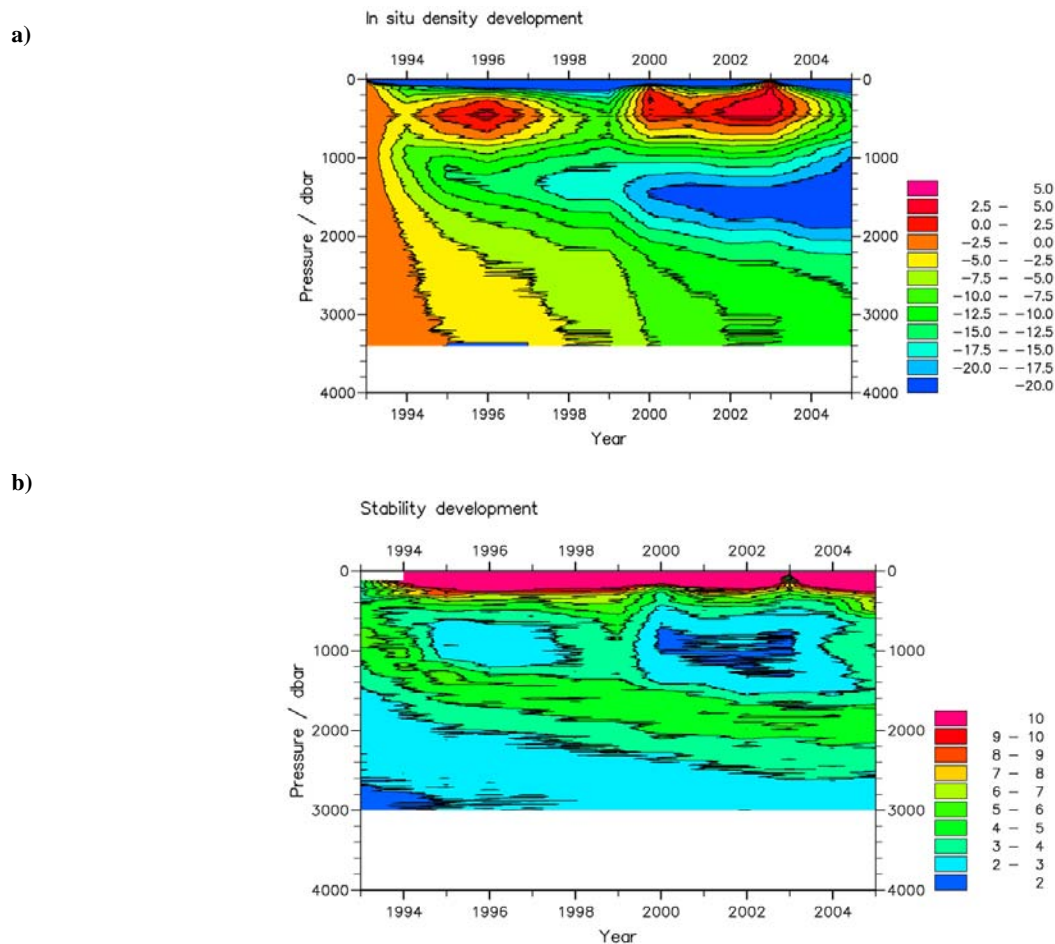


Fig. (10). Development of **a)** in situ density relative to 1993 and **b)** stability (10^{-8} m^{-1}) in the gyre centre.

restratification phase between the time of convection and that of the cruise, but dense sampling in time, including cruises directly after the convection phase, document the intact stratification [26]. Below the annually varying depth of winter convection, the stability in the upper layer has a tendency

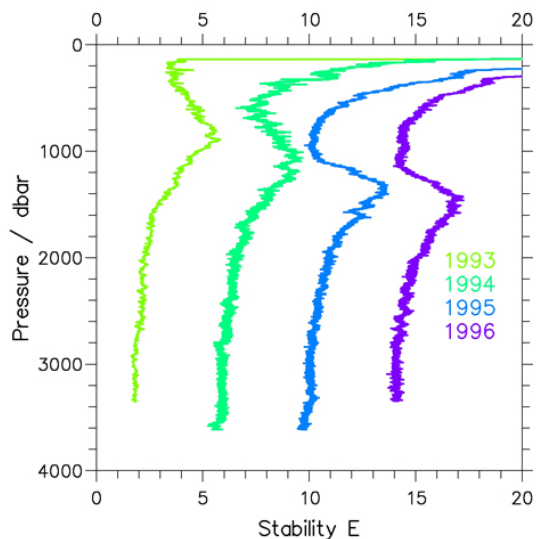


Fig. (11). Stability profiles (10^{-8} m^{-1}) from 1993 through 1996 in the gyre centre.

to increase with time due to advective contributions/modifications.

In summary, a general trend is also not apparent in the stability development of the upper layer, and there are several phases of stability increase and decrease in the investigated period which are related to the respective convection type and convection depth in winter. The general structure with a stability maximum at the interface, which is more or less prominent due to the interplay of advection and winter convection, persists during the entire time series and in particular we do not recognise a dramatic change in stratification between 1994 and 1995 as proposed by [23] but observe rather consistent conditions during that period (Fig. 11). A rapid descent of the interface is observed then, and any construction of means over several years will smear out the vertical structure.

THE INTERFACE

The characteristic feature of the two-layer structure is the interface between upper and lower layer at mid depths. It is defined by outstandingly large vertical gradients in salinity, σ_0 and a large number of chemical as well as biological parameters (e.g. concentrations of nutrients, oxygen, CFCs, nanoplankton, bacteria abundances etc.). These gradients are accompanied by an intermediate vertical temperature maximum and the aforementioned stability maximum. The two

parted structure extends laterally from the Arctic Front, situated between 5 and 10°E, and the beginning of the East Greenland bottom slope at about 8°W (see any figure of Fig. 2 and 3). At least from 1993 up to today this structure prevails. However, its interface is observed at steadily increasing depth levels: From roughly 900m in 1993 it descended to 1800 m in 2003.

This displacement has, self evidently, to be taken into account when constructing time series covering a certain vertical extent. Typical properties of the upper or lower layer cannot be calculated as averages over fixed depth ranges but must regard the displacement, as the descent of the main gradient will otherwise dominate the changes. Note also, that the depth of the interface in a particular year is not level but shows a local variability in the range of 200 m (CVs excluded), so that a larger number of stations is needed to define the interface depth of the background. The scatter in the descent of the temperature maximum (see below, EP/CC-Jojo) and in the transect plots demonstrate this variability (see e.g. salinity in 2000).

Origin

It poses somewhat of a problem to date the establishment of the two-layer structure, because the first years in the 90s are characterised by a severe lack of field data due to the phase-out of the Greenland Sea Project (GSP). We know that the structure was fundamentally different from the actual one and similar to the one shown in Fig. (5) still in 1989 [29] when extensive cruises have been performed. Thus we make an attempt to trace back the situation from 1993 to 1989 on the basis of occasionally taken profiles. For 1993, we know that the two-layer structure had already developed (compare Fig. 2). For 1991, a single station performed in the Greenland Gyre already shows a low salinity layer with salinities below 34.88 over a vertical extent of 400 m (Fig. 12). Also, the later prevailing temperature maximum is apparent, though at higher temperatures than during the period after 1993. The pool of very low temperatures above it indicate convection to only about 400 m or less in the previous winter. Further back in time, in 1990, most profiles in the central

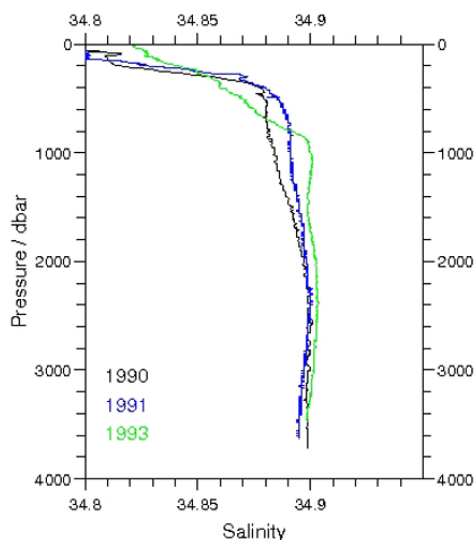


Fig. (12). Salinity profiles in the gyre centre (single profiles) from 1900 through 1993.

Greenland Sea exhibit a similar low salinity top layer with salinities below 34.85 of about 200 m depth (an example is included in Fig. 12). A basin wide temperature maximum in the salinity gradient is also established in 1993. Again, the very low temperatures above it indicate only very shallow convection in the preceding winter.

Thus, the establishment of the 2-layer structure has to be dated to the period between 1989 and 1990. During this time, no exceptional fresh water transport is identified in model simulations of the EGC [27], but the difference between Fram Strait and Denmark Strait fresh water transports shows a singular maximum in the 50 year long simulation. This corroborates that a distinct fresh water input into the Greenland Gyre must have occurred then and that several years of very shallow winter convection formed an upper layer of relatively low density with a strong gradient at its lower boundary thereafter. This event altered both the basin wide structure and the conditions for convection fundamentally, as an effective downward limit for convection is established. The rapid rearrangement from 1989 to 1990 has been noted before [29], its overwhelming importance and its persistence, however, can only be judged from today.

Development

The accrument of the temperature maximum is related to the formation of the two-layer large scale structure. The uppermost, relatively fresh, waters have been cooled in an environment with a negative downward temperature gradient (warm at top, cooler with increasing depth). Its recent temperature has been settled only after a longer formation phase: Shortly after its first appearance, in 1990 and 1991, the intermediate temperature maximum is located rather shallow and shows relatively high temperatures when compared to later years. Due to its provisional shallow position, it is subject to modifications by surface forced processes. Initially, its temperature is developing towards lower values. This can readily be explained by the combined effect of wind stirring and winter convection, which homogenises the upper water column and gradually entrains the underlying waters. A local temperature maximum still remains after that, but its temperature is reduced. According to this formation process, the temperature maximum is located at the downward limit of the salinity/density gradient of the interface. In 1993, the temperature maximum shows values slightly above -0.85°C . The layer with temperatures warmer than -0.85°C prevails then during the entire time interval discussed here and has not been interrupted during any winter.

After the establishment phase, the interface's temperatures remain remarkably constant which contrasts the development above and below it. The temperature maximum values vary in the small range between roughly -0.84 and -0.82°C during the period from 1993 to 2005 (Fig. 13). This indicates that the vertical exchange at this depth is rather small, as otherwise the temperature maximum would be eroded measurably in a short time.

Some erosion from above, caused by winter convection, can be recognised during winters when convection reached down to the density step. A very slight temperature reduction might be recognised between 1994 and 1995, but a more pronounced reduction of 25 to 30 mK (from about -0.82 to -0.845°C) occurs between 1995 to 1996. A comparison with

the specified convection depths reveals that during both winters convection penetrates to the density gradient and is apparently strong enough to erode small bits of the temperature maximum. During the following years, the temperature maximum value increases slowly by roughly 5 mK per year. After 5 years, in 2001, the temperatures scatter again around -0.82°C . This is possible because the temperature maximum is not affected by winter convection during this entire period: convection depths are clearly shallower than the depth level of the interface from 1997 through 1999, and convection does not penetrate to the high salinity end of the density step in 2000 and 2001. In both following years, 2002 and 2003, the value of the temperature maximum is reduced again (by the order of 5 mK), due to the effect of convection.

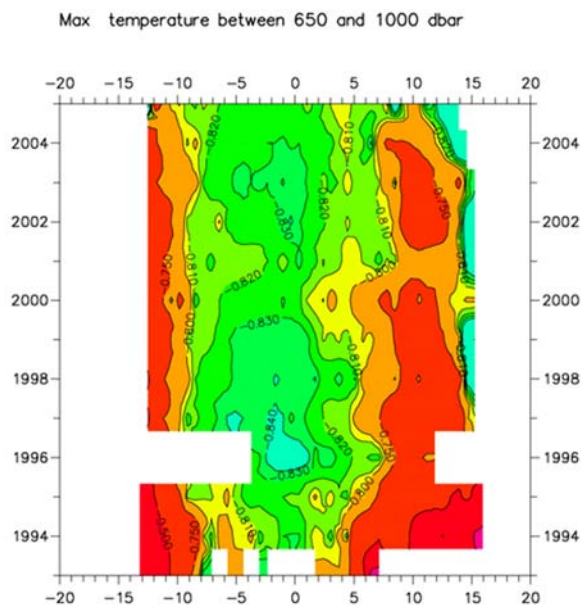


Fig. (13). Development of the maximum temperature in the interface from 1993 to 2005 over the entire zonal transect between 20°W and 20°E . The vertical range of the layer which is evaluated by the search algorithm is moved with the descent of the interface. Apparent changes in the Atlantic Water domain are due to this shift exclusively. The focus of the plot is on the cold domain in the centre.

The observed changes are very small and often difficult to estimate. Nevertheless, the fact that temperatures increase at all under undisturbed conditions indicates that there must principally be a lateral input into this layer as the waters above and below are colder and cannot serve as a heat supply.

Consistent with the described accrument, the intermediate temperature maximum is combined with the high salinity end of the salinity/density gradient. During the descent of the interface, this relation between the temperature maximum and the salinity/density step remains fixed. However, the salinity at the temperature maximum is not exactly constant but increases slowly but steadily with time. This development is in accord with that of the lower layer (see next chapter) and indicates a connection of the waters in the interface to the deep Arctic water components at the rim. Various authors showed that the properties of the Canadian Basin Deep Water (CBDW) closely resemble those in the interface

[30-32]. Of course, this does not mean that the establishment of the interface was caused directly by an inflow of CBDW. Rather, winter convection distributed fresher and colder waters vertically in a warmer and more saline environment down to a density level which coincides with that of the CBDW. Lateral exchange on isopycnals subsequently takes place between the CBDW and the interface waters in the gyre centre and hereby maintains the interface's temperatures.

Descent

The descent of the gradient is a process of particular interest. During the first part of the time series, the interface descends rapidly and steadily while during the later part the speed of the descent is reduced. The vertical position of the interface can best be determined by the temperature maximum in the contour plots (when classes are chosen appropriately), or the salinity and density step in the profiles. It is important here to identify CVs and to distinguish between background and CVs. CVs (apparent in 1994, 1997, 2001, 2002) lead to a downward displacement of the interface of several hundred metres, but also profiles measured at their rim introduce vertical scatter. A sufficient number of stations is therefore indispensable to be able to distinguish between the background and the eddies, but it might still be difficult to quantify small descents of the interface due to the vertical scatter. The main development of the interface's vertical position, however, is readily evident from the time series: From a depth of 900 m in 1993, it has descended to a level of 1800 m in 2003. A tentative list of its progression in time is 1994: 1050 m, 1995: 1300 m, 1996: 1400 m, 1997: 1400 m, 1998: 1500 m, 1999: 1500 m, 2000: 1600 m, 2001: 1700 m, 2002 to 2005: 1800 m. It is evident that this list is disparate to the opinion that the temperature maximum remained static at 1500 m from 1995 onwards [23,33] at least until 2002 the descending phase continued.

In the most recent years, the interface forms a depression in the central gyre, which is apparent in all hydrographic parameters (see Figs. (2), (3), (4); 2003 and later). This shows that its descent is not due to a relaxing of the former doming structure [34]. While the forcing of the descent is not resolved to date (and our best numerical models actually do not show such an interface yet), it is possible to check for direct dependencies on the basis of available field measurements.

The descent of the interface could principally be caused by an erosion from above (winter convection), or alternatively by an advective vertical shift. From the salinity or density field it is not possible to decide whether convection erodes the density step or if, vice versa, convection extends deeper over the years because of the descent of the step. It is the temperature field which corroborates an advective shift. After 1993, the interface undergoes a vertical displacement of almost 1 km. A related erosion, with other processes neglected, would modify the temperature maximum from -0.85 to about -1.1°C . As already shown, such an erosion of the temperature maximum is not observed. At places where erosion occurs, it can clearly be recognised: The decrease of the maximum temperature (together with a sharpening of the temperature gradient) is apparent in the core of CVs, and, to a much lesser extent, during the years with convection down to the interface also in the background.

Occasionally a causal link between winter convection and the interface descent is discussed [23]. This is not corroborated by our time series. A comparison between convection depths and the interface's vertical displacement shows no direct relation between convection and interface displacement. During years without deep convection, the interface may descend markedly (as in 1997/98), but during years with deep convection the descent may be small or vanishing (as in 1996/97). A more perspicuous indicator stems from two-daily CTD profiles performed by an autonomous deep sea profiler (EP/CC Jojo, 2000 to 2001) over an entire year. These measurements show that the interface's descent (here characterised by the depth of the temperature maximum) is not related to a certain season, and in particular not to the winter period, but occurs steadily with time (Fig. 14).

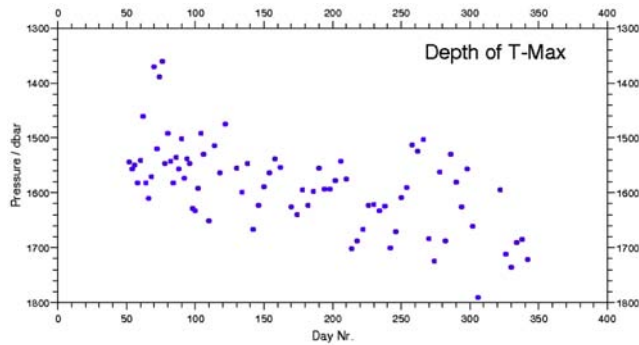


Fig. (14). Depth of the temperature maximum from an autonomous CTD-profiler in the gyre centre. Start day is 19.7.2000.

THE DEEPER LAYER

With the absence of bottom reaching convection, the lower layer in the Greenland Sea remains essentially isolated from atmospheric and upper ocean influences. No dense waters are formed on the shelves of the Greenland Sea (including the vast area of the Northeast Water polynya in Fram Strait), and the dense and salty outflow of Storfjorden flows northward so it does not reach the Greenland gyre. The fact that the Greenland Basin is surrounded by a ridge system -

with depths only slightly more than about 2000 m and only some troughs reaching deeper-contributes to the isolation of the lower layer: The deepest waters in it cannot be reached by isopycnal exchange.

The vertical isolation of the deeper layer is demonstrated perspicuously by the actual oxygen distribution which shows a distinct boundary between the ventilated upper and the isolated lower layer (Fig. 15). Despite this vertical isolation, the hydrographic properties of all deep waters in the lower layer change continuously. The most robust trend is the temperature increase, which is always evident no matter what depth is considered, and whether or not means over depth ranges are used. This trend is reflected in the transect plots which further show that many temperature class limits are shifted downward in pace. A detailed analysis will reveal exceptions, but for the overall trend within the time period investigated here, the statement is valid.

The salinity development is more intricate. Interannual differences are at the limit of present day accuracies, but the long term trend reveals a clear signal to higher salinities. It is evident that lateral exchange with the rims introduces more salty deep Arctic waters into the gyre, but salinities increase also below their densest isopycnic surface. Thus, vertical processes apparently play also an important role in modifying the deep waters. Without winter convection penetrating into the deeper layer, the modifications due to both lateral and vertical processes act without interruption for a long time span, facilitating their detection.

Stability in the deeper layer is small, and the vertical temperature differences in it are large enough to make the shape of the density distribution highly dependent on the choice of the reference pressure level.

Due to the vertical descent of the interface, the deeper layer's volume is reduced substantially in the course of the time series. With the interface located at 900 in 1993 and at 1800 m in 2003, about 1/3 of its 1993 volume is lacking in 2003. (Related to the previous cold water dome reaching to the surface, the deep water volume is reduced to roughly 50% in 2003.) The volume reduction from 1993 onwards

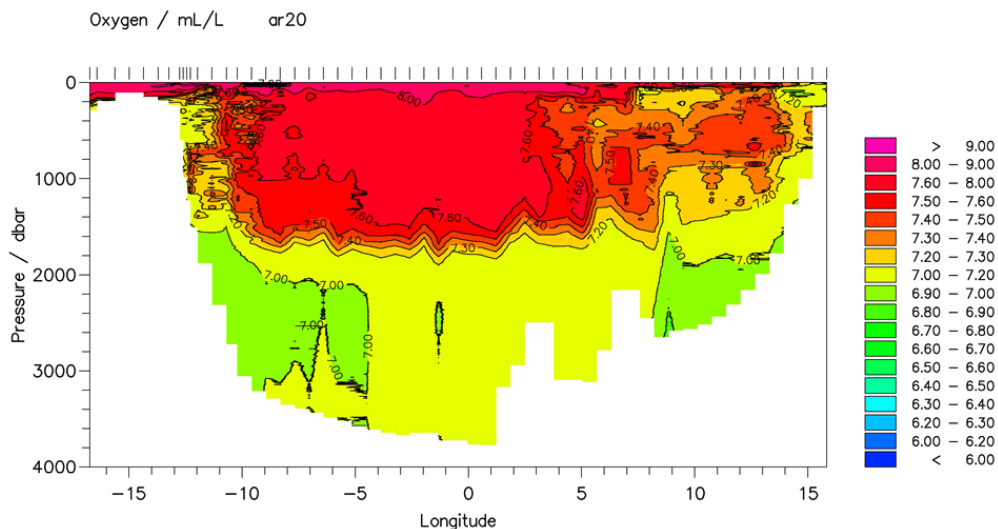


Fig. (15). Oxygen content distribution (mL/L) on the zonal transect at 75°N in 2004. Data stem from profiles with an SBE43 electrical oxygen sensor; their accuracy is estimated to 0.2 mL/L.

must be combined with an export from the deeper layer. It is shown below that this export takes place in a boundary layer close to the bottom.

Temperature Development

In the beginning of the time series, the temperature shows vertical as well as lateral gradients in the deeper layer, as it contains the remnants of the previous cold water dome. In 1993, the bottom temperatures are below $\theta = -1.2^\circ\text{C}$ and the -1.00°C isotherm shows a doming of about 600 dbar. After the establishment of the upper layer and its subsequent volume increase caused by the interface descent, the isotherms in the gyre are level in 1997 or 1998. The isotherms $\theta = -1.15^\circ\text{C}$ and $\theta = -1.00^\circ\text{C}$ approach the bottom steadily in the entire basin until the class limit of $\theta = -1.15^\circ\text{C}$ disappears in 2000 (see Fig. 2a-h and Fig. 16). The cold water pool with temperatures below -1.10°C disappears in 2003 (Fig. 16).

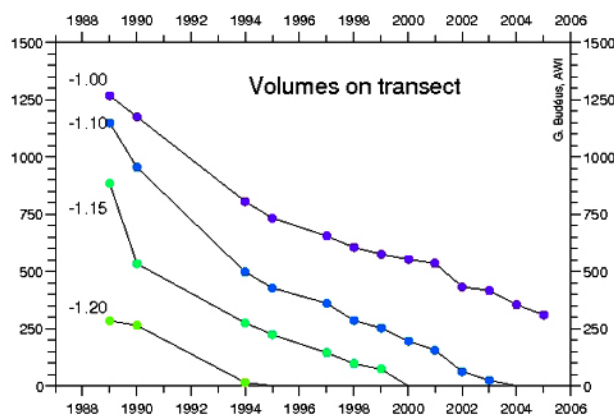


Fig. (16). Volume of water with temperatures below the indicated threshold on the zonal transect (km^3 , 1 km width times area on transect) from 1989 through 2005.

A remarkable feature of the temperature development is the fact that temperatures do rise not only at the bottom or within a restricted depth range of the lower layer but at all depth levels below the interface while this is descending (Fig. 7). Only few exceptions from this are observed. Between 1993 and 1996, temperatures increase steadily and rapidly combined with a rapid descent of the interface. From 1996 to 1997 no detectable interface descent is observed, and temperatures remain constant in the entire deep layer. Note that in Fig. (8) both isotherms at $\theta = -1.10^\circ\text{C}$ and $\theta = -1.15^\circ\text{C}$ remain at constant depth levels then. The overall temperature increase continues between 1997 and 1998. Only small temperature differences are observed between 1998 and 1999, when the interface remained static, too. Between 1999 and 2002, descent and temperature increase continue again. After 2002, the development is structurally different from the preceding period: Between 2002 and 2003, the temperature difference below the interface is vanishingly small over most of the deeper layer's depth range. Only close to the bottom a temperature increase is observed, and this will be used below to estimate the strength of vertical diffusion. Between 2004 and 2005, a similar situation is found with zero temperature increase directly below the static interface level but differences growing larger with depth.

The temperature increase is not consistent with the inflow of deep Arctic waters (which are responsible for the for the

salinity modifications, see below) as is proposed by [23]. Lateral temperature gradients on the deep isopycnic surfaces are negligible since 1995, and during the later part of the time series, temperatures at pressure levels or on deep isopycnic surfaces are even lower at the rim than in the gyre's interior due to the recent depression of the interface and the upslope trace of the cold bottom waters.

An important question is, whether the temperature increase occurs steadily within a year, i.e. if it is independent of seasonal processes - in particular of winter convection -, or if it shows an episodic nature. Both near bottom temperature measurements (1998/99, not shown) as well as a deployment of an autonomous profiler (summer 2000 to summer 2001, shown in Fig. 17) show that the temperature increase occurs not episodic but steadily over the entire year. This suggests a continuous process as the cause of the temperature development, in particular independent of winter convection. A steady descent of the water column or alternatively continuous diapycnal mixing are proposed as candidate processes. We do regard the first as the dominating process during the first part of the time series and discuss the effects of both further below.

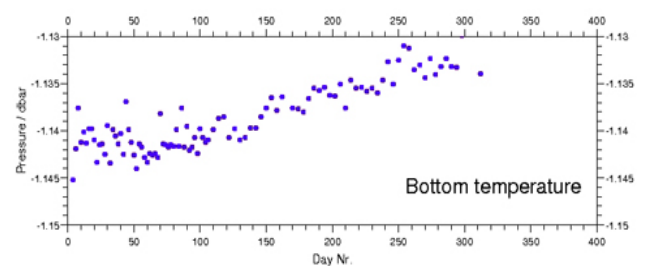


Fig. (17). Bottommost potential temperature from an autonomous CTD-profiler in the gyre centre. Start day is 19.7.2000

Salinity Development

While the interannual salinity increase in the central gyre is not resolved by actual salinity accuracies, but the long term salinity increase represents a clear signal and is consistently reported by various researchers [21-23,35]. Between 1993 and 2005, the increase of the salinity maximum in the deep waters amounts to 0.01 (34.902 in 1993, 34.912 in 2005).

In 1993, 1994 and 1995 a slightly fresher layer exists between two salinity maxima, one of them at about 1000 m as part of the interface and a second, slightly more saline, at roughly 2400 m. The upper maximum descends together with the interface and the temperature maximum (Fig. 7 and 8). Similarly, the high salinity values at the lower maximum progress towards the bottom, as can be seen e.g. from the 34.905 isohaline between 1997 and 2002 (Fig. 3e-j and 8). The initial vertical structure with the double salinity maximum disappears in the course of the time series: Between the two maxima which are present between 1993 to 1995, a slightly faster salinity increase is observed than at the depth ranges of the maxima themselves. This leads to one broad salinity maximum layer which exists from 1996 onwards and incorporates the two former maxima and the volume between them. The continuous broadening of the high salinity layer (Fig. 8) indicates that there is not a merg-

ing of the initial two salinity maxima in a sense of a mutual physical approach and an export of waters between them.

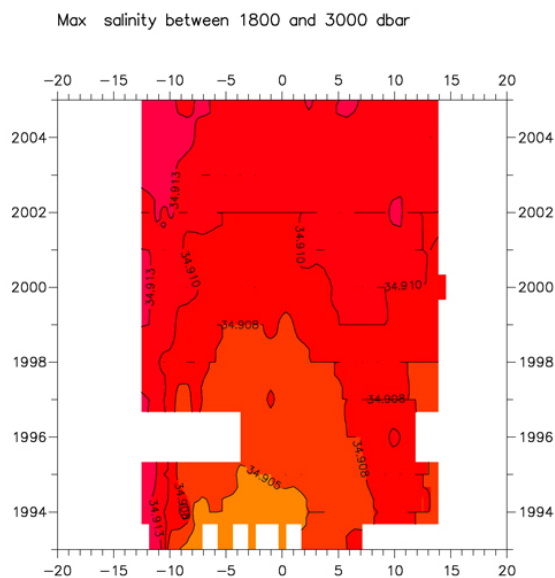


Fig. (18). Development of the maximum salinity between 1800 and 3000 m from 1993 to 2005 over the zonal transect between 20°W and 20°E.

The input of high salinity waters can be identified due to the transects' extent: It occurs from both rims in the west and in the east and is attributed to the Deep Arctic outflow which flows around the Greenland Basin. The salinity increase occurs first on the western side of the basin and with a delay at the eastern side, where the higher salinities appear at Mohn's Ridge (Fig. 18, e.g. $S=34.910$ in 1999). The temporal succession of the 34.905 isohalines' position moves from the rims in 1994 towards the centre in 1995 (see also Fig. 3b and c). In 1997, waters which are more saline than this threshold fill a laterally uninterrupted layer across the entire basin. Already in 1995 no water is left in the deeper layer of the Greenland Gyre which would have been specified as GSDW during the 80s as a consequence of the increase in salinity above the class limit of 34.900. A similar progression from the rims to the centre is observed between 1999 and 2004 for the 34.910 isohaline. The successive progression of both the 34.905 and the 34.910 isohaline shows first that the transfer of properties from the rim into the gyre's centre is important for the development in the interior, and second that this is a slow process which takes a number of years for the propagation of a signal from the rim into the centre. Lateral gradients in the deep layer are not reduced rapidly but are maintained over many years.

Overall, the salinity development in the deeper layer is dominated during our time series by the uninterrupted spreading of the rim water masses into the gyre centre. In addition to this salt input, the entire salinity structure descends; an ascent of the deep salinity maximum, as proposed in [23], is not apparent.

The existence of only one salinity maximum in the late 90s is consistent with the salinity distribution at the rim, where homogeneous salinities are found in a depth range between 1500 m and 2700 m. The shape of the TS-relations in the deep EGC does not show two maxima for any of our

cruises between 1995 and 2004. This means that an influence of an EBDW salinity maximum is not apparent, which stays in contrast to previous propositions that an import of EBDW explains the two salinity maxima in the deep layer of the Greenland Sea, reported for the 80s and evident until 1994, is then not the result of an EBDW import but rather due to preceding convection events: both salinity maxima would be formed in the same fashion, namely by a vertical input (winter convection) of fresher waters into a more saline environment (comp. [23]). This complies with a downward vertical fresh water flux as it is associated with the classical view of Greenland Sea winter convection (and which is not always realistic today) together with a convection which is limited to intermediate depths.

Vertical Processes and Deep Water Export

Vertical (diapycnal) mixing has been discussed on various occasions as a potential candidate for the explanation for deep water changes, in particular for the temperature increase [34,37] and there have been several attempts to quantify vertical mixing coefficients [2,3,38] in different parts of the Greenland Basin. [2] evaluated the tracer experiment (SF-6) and proposed a vertical exchange coefficient k_v between 0.1 and $1.4 \cdot 10^{-3} \text{ m}^2/\text{s}$ for the layer occupied by the tracer. This was, and still is, the upper layer of the two parted structure, and consequently this value includes the effects of convection. An estimate for the deep layer was proposed on the basis of an accidentally dropped SF-6 volume and amounts to about $0.8 \cdot 10^{-3} \text{ m}^2/\text{s}$ [39]. Two studies based on LADCP measurements estimate elevated values in the deeper parts of the basin at the bottom (k_v about $5 \cdot 10^{-3} \text{ m}^2/\text{s}$ [38]) or alternatively in the interior (k_v about $80 \cdot 10^{-3} \text{ m}^2/\text{s}$ [40]).

When regarding vertical exchange alone, it has already been proposed [35] that locations in the interior would, to a first approximation, neither gain nor lose heat by vertical mixing because of the similar temperature gradient against depth which leads to a depth independent heat flux when constant exchange coefficients are assumed. Heat would accumulate only at the boundary and a homogeneous boundary layer of increasing thickness would be established. Such a continuous long term homogenisation of the deep waters is not observed.

For short periods, however, the above scenario is apparent. As an exception from the general temperature trend in the deep waters, the development between 2002 and 2003 shows a stationary interior temperature profile with no descent of the temperature maximum and no general temperature increase below it. Only the bottommost part of the water column shows increasing temperatures then. Together with this, a vertical homogenisation is observed in the layer close to the ocean bottom (Fig. 19). This is the expected result if the heat conduction problem with one isolated side (here: at the bottom) is considered and so it is possible to quantify the vertical mixing coefficient in the deep waters from the hydrographic development itself.

Assuming that the observed warming took place steadily over the time span of one year, the relation between the accumulated heat (5 mK mean temperature change in a 400 m thick layer) and the prevailing temperature gradient (0.1 K

per 1000 m) leads to a k_v of $0.7 \cdot 10^{-3} \text{ m}^2/\text{s}$. This fits remarkably well to the estimate derived from the accidental SF-6 drop and corroborates such a relatively high deep sea value. A likewise progressing vertical homogenization of the bottommost waters should occur when further vertical mixing is applied. As such a development is lacking, we have to conclude that diapycnal mixing is not the main reason for the deep water modifications on the long term. Another inconsistency would arise from the assumption that internal mixing alone is responsible for the observed modifications: It would have to have ceased suddenly during the year of the above example (2002 to 2003) in the interior of the deep layer, but not close to the bottom.

Once accepting that the development in the lower layer cannot be explained without a main contribution by vertical advection (which includes the interface), a net outflow in the deeper part and a net inflow in the upper part is requested. While it has been shown that a surplus of AW is needed to describe the processes in the upper layer correctly, the net outflow in the lower layer has not yet been observed directly. The SF-6 drop could potentially identify a pathway, but no material is published yet with respect to this.

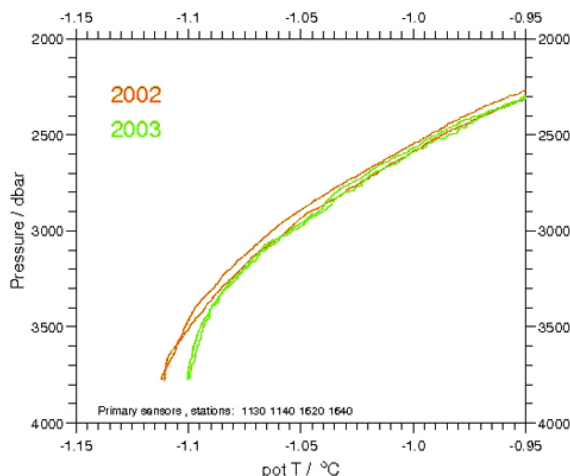


Fig. (19). Temperature increase in the bottommost waters between 2002 and 2003 from the two profiles closest to the Mohn's Ridge each year.

Therefore we must rely on indications to identify at which depth level this export takes place. [23] propose that the export occurs in the upper part of the deeper layer and that the volume between the two salinity maxima is squeezed by this process. This is probably guided by the misconception that the deep salinity maximum rises during the time series while the upper maximum moves downwards until both merge. Figs. (5 and 6) show that the salinity development is fully consistent with the idea of vertical advection, as the entire salinity structure descends similar to the temperature structure. The temperature development itself provides a strong argument for an export close to the bottom: The lacking progressive homogenization of the bottommost waters can be avoided with an export at this level. The homogenized bottom boundary layer would be included in the export and would have to be maintained continuously against the vertical advection of stratified media.

In order to identify possible export processes or contradictions to it, it is useful to inspect isotherms at the rims in

detail. At the eastern boundary of the gyre, we recognise that isotherms hit the Mohn's Ridge mostly without vertical excursions. This stays in contrast to the structure which is to be expected when substantial vertical (diapycnal) mixing acts: A homogenization of the lower layer with downward bending isotherms would be the result. At the western rim, too, a downward bending of isotherms is not apparent. In contrast, upward tilting of the bottommost temperature class is often observed. The occurrence of this feature during many years of our time series shows, that this is not a transitional but a regular feature of the boundary layer there. In accord with [32] and [41] we interpret this as an uplifting and export of bottom waters at the slope.

CVS

An overview of the Greenland Sea's hydrography in the 90s and later would lack completeness if the occurrence of CVs was not included. Their relevance for the hydrographic development in the background is the aspect which is covered here, while their properties are only summarised, because they represent only a small fraction of the basin's total water volume, and extended literature exists which deals with their hydrography and dynamics [18-20,42,43].

CVs are characterised as vertically more homogeneous features in a comparatively more stratified environment [44]. Those observed in the Greenland Sea possess diameters of about 20 km and rotate anticyclonically. To a first approximation the rotation is solid body like and extends to great depth. Maximum velocities amount to about 25 cm/s. The part above the density step is not only less stratified than the surroundings, but often also of remarkable homogeneity. Their core is less saline and colder than the surroundings. Although it may be suggestive, this alone does not indicate a formation during winter. It is sufficient to incorporate a lower amount of AW into the SCV core than into the surroundings to establish this difference. Several observations show that the core of an SCV is apparently well separated from the surroundings [18,19].

Within an SCV core, the homogeneous upper part does not 'penetrate' through the temperature maximum layer as is occasionally suggested from plots of coarsely sampled CVs, but the salinity/density interface is only displaced up to 1000 m deeper than in the background. The TS-relation below this step remains intact and resembles that of the background. Only the coldest part at the bottom might be lacking (thus producing a slightly warmer 'bottom shadow' [20]) and the uppermost part of the interface may be eroded by winter convection in the CV core. This is similar to the situation in the background, where winter convection also may erode the upper part of the interface during some years when winter convection extends deep enough. The intermediate maximum temperature is then slightly decreased, in the background as in a CV.

Due to the lower stratification inside a CV (Fig. 20), winter convection can reach here to greater depths than in the background, and the CV core may be ventilated down to the density step also during winters with only moderate ventilation depths in the background. As a CV seems normally to be open to the surface in winter (see [20]), substances exchanged across the ocean surface are transported to the largest depths at these sites. As the interface between the upper

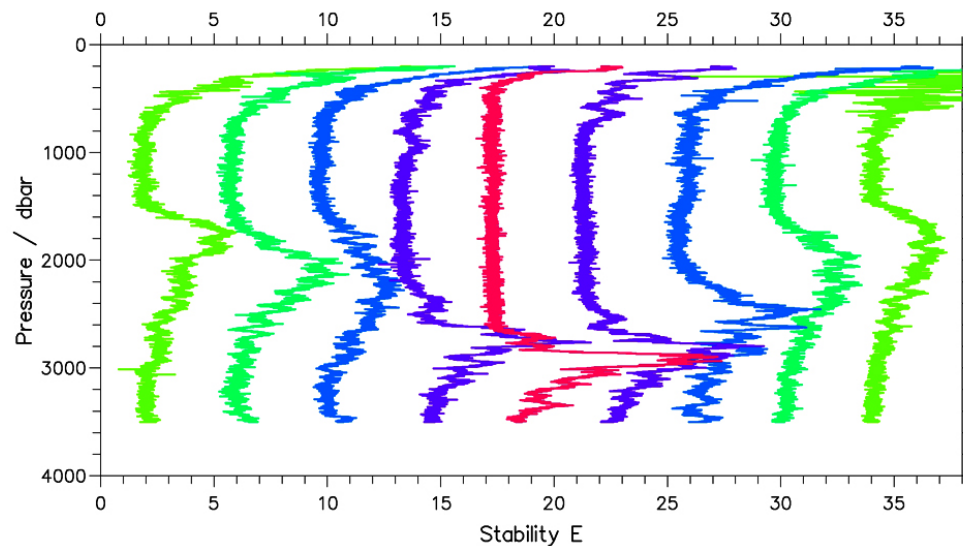


Fig. (20). Stability profiles (10^{-8} m^{-1}) on a transect across a CV. Overall distance between the outer profiles is 22 km with equal distances between the stations. Centre is $75^{\circ}00.45' \text{ N}$ and $00^{\circ}47.32' \text{ W}$. Observation was performed on July, 24th, 2002. The scale is for the first profile, offset of subsequent profiles is $4 \cdot 10^{-8} \text{ m}^{-1}$ each.

and lower part descends in the CVs similarly to the background, the well ventilated waters are only 900 m from the ocean bottom nowadays (interface at 2700 m in a CV vs. 3600 m water depth in the central gyre).

CVs have been identified only recently in the Greenland Sea, mostly because of their small size, and are regarded as a phenomenon novel of the late 90s. First reports are presented in 2002 [18] and refer to observations during 1997, but in 2005 [23] presented a CV observation as early as 1993. Browsing through our own time series, we identify 2 CVs in 1993 in accordance with the latter report. In the later years we met one or more in 1994, 1997, 2001, 2002, 2003, 2004, and 2005 on the transect or close by, partly after searching for such a feature.

Within the scope of this paper these features seem of minor importance since they do not represent large water volumes of the Greenland Basin. However, a problem arises from the fact that stations within a CV are often included in averages of the Greenland Sea properties. As is immediately evident, an inclusion of an SCV in an average will deteriorate the mean properties considerably, with regard to typical properties as well as to gradients and the existence of local extremes. The intermediate waters (upper layer of the two part structure) will be biased towards colder and fresher values. The temperature maximum layer, the stability maximum and the salinity/density step will have a tendency to disappear. And the deep waters will show a bias towards higher temperatures. Knowing that CVs are small and form exceptions from the background conditions, they should be identified and excluded from a background analysis. With a sufficient number of stations it is easy to identify them from the density field (see e.g. 2002 in Fig. 4), where isopycnal surfaces in the upper layer are located shallower, but in the lower layer are located deeper than in the surroundings of a CV. This discriminates them from other eddies with parallel shifts of the isopycnals.

It is possible that the sparseness of hydrographic stations previous to the 90s is adverse to their detection before. The

few examples of CVs presented here can evidently not replace a more complete scanning of the existing data pool for their occurrence. It seems a worthwhile effort of its own to undertake such an investigation.

INTEGRAL VIEW

From the presented material it is evident that the situation in the Greenland Basin during the last decade is fundamentally different from that before which was characterised by a huge cold dome in the gyre's centre. The most important aspect of its present hydrographic structure is the stable vertical interface which establishes a two layer system and parts the waters in an upper and lower layer. It is presumably triggered by a fresh water input anomaly in 1990 which is not associated with a high Fram Strait transport and demonstrates that a temporal anomaly of the regional fresh water distribution may lead to persistent structural changes in the ocean. The vertical interface and the two layer structure prevail until today.

Due to a descent of the interface, the volume of the deeper layer decreased by roughly 50% with respect to the 1993 state. There is a number of indications that the necessarily associated export in the deeper layer takes place close to the bottom and is concentrated at the western side of the basin. This means that the concept of a descent of the entire water column in the central gyre is corroborated by the presented time series. The energy needed to lift the deepest waters to a level suited for their exportation can be supplied by the strong rim currents and its amount is not different from that which would be needed for diapycnal mixing in the interior. It is clear that the exported waters take their vorticity with them (as it is a Lagrangeian property) and so we expect no vorticity rearrangement in the Greenland gyre as discussed by [23].

During the actual two-layer phase, the deeper layer is isolated from surface influences. Thus, it continuously increases in age and is hardly ventilated. However, lateral exchanges with other water masses result in property changes.

The deep Arctic outflow surrounds the Greenland gyre and has a determining influence on the waters in the deeper layer of the Greenland Basin. Vertical exchange in the deeper layer (diapycnal mixing) is also apparent in the course of the time series. It plays a minor role during its first part, can be quantified during the later part and may be of increasing relative importance if the descent of the interface is ceasing more permanently.

Thus, three processes combine their effects in modifying the deeper layer: the descent of the water column (and the related export), vertical exchange, and lateral exchange. The development of the different hydrographic properties is dominated by different processes. This is due to the respective property distribution, i.e. to the direction and strength of the main gradients. While the salinity development is dominated by lateral exchange but cannot be fully explained without vertical advection, the temperature development is dominated by the water column descent and shows additional influences of vertical mixing. The density development cannot be explained by isopycnal mixing but is indicative for vertical advection. The developments of the different parameters show that all three effects are important for the recent hydrographic modifications.

The most important effect of the interface is that it serves as a barrier against a deep penetration of winter convection. The property development in the interface itself shows only minor changes, but these indicate that some restoring influence must act. As all properties resemble those of the CBDW, a lateral exchange with this water mass must be the responsible process. The present connection to CBDW is not synonymous with a direct establishment of the interface by these waters.

The function of the interface as a barrier against ventilation is varying in relevance. When the upper layer is vertically homogeneous, it is indeed the first stability barrier met by winter convection. When the upper layer is substantially stratified, the entire layer hampers deep reaching convection. The time series shows that the upper layer can occasionally be stratified in a manner that the interface is only barely recognised as a stability maximum. This does not lead to a general cease of convection but is apparently a reversible state.

Periods of higher and lower stability alternate in the upper layer, what we attribute to the convection history and convection type. As in the deeper layer, the three effects of water column descent, vertical exchange and lateral exchange combine. However, the descent is associated with import in the upper layer, and vertical exchange is dominated by winter convection and is therefore not steady but both vigorous at times and transient. Winter convection has diverse effects on the temperature, salinity and stability development. Temperatures might increase or decrease, salinities might increase or decrease as a result of convection, and the water column might be homogenised or be left in the stratified condition which it attained by lateral exchange after a previous homogenizing event. Much of the previously unexpected effects of winter convection are due to the fact that an import of Atlantic waters is not generally adverse to convection but greatly modifies its results. By the inclusion of AW derivatives, winter convection may lead to effects which resemble those of lateral exchange.

Lateral exchange affects the entire upper layer and leads always to a temperature, salinity and stability increase. This is specific to the situation in the Greenland Basin with its rim currents and particular water masses. Lateral exchange is interrupted only where winter convection erased its signal; below this depth it simply continues. A correct analysis of the winter convection history is therefore indispensable for an explanation of water property modifications in the Greenland Basin. In the upper layer, the combined action of water column descent (and import), vertical exchange and lateral exchange is much more complex and less predictable than in the lower layer. A steady trend is not apparent in any hydrographic parameter of the upper layer during the extent of the presented time series.

The complete body of observed changes with the interface descent (which is independent of winter convection), the isolation of the deeper layer, the temperature and salinity development there, and the bottom layer export of the coldest waters corroborate the idea that a large single-cell continuous convection scheme dominates the volume changes of both upper and lower layer and the deep water modifications during the 90s.

REFERENCES

- [1] Wadhams P, Wilkinson JP, Wells SCS. Eds. ESOP European Sub-polar Ocean Programme, Sea Ice -Ocean Interaction 1996.
- [2] Watson AJ, Messias MJ, Fogelqvist E, *et al.* Mixing and convection in the Greenland Sea from a tracer release. *Nature* 1999; 401(6756): 902-4.
- [3] Messias MJ, Watson AJ, Johannesen T, *et al.* The Greenland Sea tracer experiment 1996-2002: horizontal mixing and transport of Greenland Sea Intermediate Water. *Prog Oceanogr* 2008; 78: 85-105.
- [4] Cisewski B, Budéus G, Krause G. Absolute transport estimates of total and individual water masses in the Northern Greenland Sea derived from hydrographic and ADCP measurements. *J Geophys Res C Oceans* 2003; 108: doi:10.1029/2002JC001530.
- [5] van Aken HM, Quadfasel D, Warpakowski A. The Arctic Front in the Greenland Sea during February 1989: hydrographic and biological observations. *J Geophys Res* 1991; 96(C3): 4739-50.
- [6] van Aken HM, Budéus G, Hahnel M. The anatomy of the arctic frontal zone in the Greenland Sea. *J Geophys Res* 1994; 100(C8): 15, 999-16, 014.
- [7] Rodionov VB. On the mesoscale structure of the frontal zones in the Nordic Seas. *J Mar Syst* 1992; 3: 127-39.
- [8] Quadfasel D, Rudels B, Kurz K. Outflow of dense water from a svalbard fjord in the fram strait. *Deep Sea Res* 1988; 35: 1143-50.
- [9] Manley TO. Branching of atlantic water within the Greenland-Spitsbergen passage: an estimation of recirculation. *J Geophys Res* 1995; 100: 20627-34.
- [10] Schauer U, Fahrbach E, Osterhus S, Rohardt G. Arctic warming through the Fram Strait -oceanic heat transport from three years of measurements. *J geophy research* 2004; 109(C6): doi:10.1029/2003JC001823.
- [11] Helland-Hansen B, Nansen F. The Norwegian Sea: its physical oceanography based upon the Norwegian researches 1900-1904. *Rep Norw Fish Mar Invest* 1909; 2(1): pp. 1-390.
- [12] Clarke RA, Swift JH, Reid JL, Koltermann KP. The formation of Greenland Sea deep water: double diffusion or deep convection? *Deep Sea Res* 1990; 37(9): 1385-424.
- [13] GSP Group. Greenland Sea Project - A venture toward improved understanding of the oceans' role in climate. *EOS* 1990; 71(24): 754-5.
- [14] Uchida H, Ohshima K, Ozawa S, Fukasawa M. *In-situ* calibration of Sea-Bird 9plus CTD thermometer. *J Atm Ceanic Tech* 2007; 11: 1961-7.
- [15] Koltermann KP, Lüthje H. Hydrographic atlas of the Greenland and Northern Norwegian Seas (1979-1987). Hamburg: Deutsches Hydrographisches Institut 1989.

- [16] Jones EP, Anderson JHSLG, Lipizer M, *et al.* Tracing Pacific Water in the north atlantic ocean. *J Geophys Res C Oceans* 2003; 108: doi:10.1029/2001JC001141.
- [17] Falck E, Kattner G, Budéus G. Disappearance of Pacific Water in the northwestern Fram Strait. *Geophys Res Lett* 2005; 32: doi:10.1029/2005GL023400.
- [18] Gascard JC, Watson AJ, Messias MJ, Olsson KA, Johannessen T, Simonsen K. Long-lived vortices as a mode of deep ventilation in the Greenland Sea. *Nature* 2002; 416: 525-7.
- [19] Budéus G, Cisewski B, Ronski S, Dietrich D, Weitere M. Structure and effects of a long lived vortex in the Greenland Sea. *Geophys Res Lett* 2004; 31: doi: 10.1029/2003GL017983.
- [20] Wadhams P. Convective chimneys in the Greenland Sea: a review of recent observations. *Oceanographic Marine Biol: An Ann Rev* 2005; 42: 1-28.
- [21] Bönisch G, Blindheim J, Bullister JL, Schlosser P, Wallace DWR. Long-term trends of temperature, salinity, density and transient tracers in the central Greenland Sea. *J Geophys Res* 1997; 102: 553-71.
- [22] Blindheim J, Oesterhus S. The Nordic Seas, main oceanographic features. In: Drange H, Dokken T, Furevik T, Gerdes R, Berger W, Eds. *The Nordic Seas: an Integrated Perspective*. Washington: American Geophysical Union 2005; pp. 11-38.
- [23] Karstensen J, Schlosser P, Wallace DWR, Bullister JL, Blindheim J. Water mass transformation in the Greenland Sea during the 1990s. *J Geophys Res C Oceans* 2005; 110: doi:10.1029/2004JC-002510.
- [24] McDougall TJ. Greenland Sea bottom water formation: a balance between advection and double diffusion. *Deep Sea Res* 1983; 30: 1109-17.
- [25] Ronski S, Budéus G. Time series of winter convection in the Greenland Sea. *J Geophys Res C Oceans* 2005; 110: doi:10.1029/2004JC002318.
- [26] Ronski S, Budéus G. How to identify winter convection in the Greenland Sea from hydrographic summer data. *J Geophys Res C Oceans* 2005; 110: doi:10.1029/2003JC002156.
- [27] Karcher M, Gerdes R, Kauker F, Koeberle C, Yashayev I. Arctic ocean change heralds North Atlantic freshening. *Geophys Res Lett* 2005; 32: doi:10.1029/2005GL023861.
- [28] Budéus G, Ohm K, Damm M, Plugge R. The externally powered, compressibility compensated Jojo mooring: a mechanical solution to autonomous deep sea profiling. *Deep Sea Res (Part I)* 2005; 52: doi:10.1016/j.dsr.2005.05.005.
- [29] Budéus G, Maul AA, Krause G. Variability in the Greenland Sea as revealed by a repeated high spatial resolution conductivity-temperature-depth survey. *J Geophys Res* 1993; 93(C6): 9985-10000.
- [30] Rudels B. The thermohaline circulation of the Arctic ocean and the Greenland Sea. *Philosophical Transactions: Phys Sci Eng* 1995; 352: 287-99.
- [31] Meincke J, Rudels B, Friedrich HJ. The Arctic ocean-Nordic seas thermohaline system. *ICES J Mar Sci* 1997; 54: 283-99.
- [32] Rudels B, Björk G, Nilsson J, Winsor P, Lake I, Nohr C. The interaction between waters from the Arctic Ocean and the Nordic Seas north of Fram Strait and along the East Greenland Current: results from the Arctic ocean-02 expedition. *J Mar Syst* 2005; 55: 1-30.
- [33] Karstensen J, Schlosser P, Blindheim J, Bullister JL, Wallace DWR. On the formation of Intermediate water in the Greenland Sea during the 1990s. *ICES Mar Sci Sympos* 2003; 219: 375-7.
- [34] Meincke J, Rudels B. Greenland Sea deep water: a balance between convection and advection. In: *Nordic Seas Conference*. Universität Hamburg 1995. Extended Abstract.
- [35] Budéus G, Schneider W, Krause G. Winter convective events and bottom water warming in the Greenland Sea. *J Geophys Res* 1998; 103(C9): 18 513-27.
- [36] Aagaard K, Fahrbach E, Meincke J, Swift JH. Saline outflow from the Arctic ocean: its contribution to the deep waters of the Greenland, Norwegian, and Iceland Seas. *J Geophys Res* 1991; 96(C11): 20, 433-20,441.
- [37] Visbeck M, Rhein M. Is bottom boundary-layer mixing slowly ventilating Greenland Sea deep water? *J Phys Oceanogr* 2000; 30: 215-24.
- [38] Garabato ACN, Oliver K, Watson AJ, Messias MJ. Turbulent diapycnal mixing in the Nordic Seas. *J Geophys Res C Oceans* 2004; 109: doi:10.1029/2004JC002411.
- [39] Watson AJ, Messias MJ, Fogelqvist E, *et al.* Long term temperature and salinity trends in the central Greenland Sea. In: Jansen E, Oheim V, Eds. *European subpolar ocean program (ESOP-2) The thermohaline circulation in the Greenland Sea - final scientific report, Appendices*. Bergen 1999. pp. a2.2 1 - a2.2 9.
- [40] Walter M. Warming of Greenland Sea Deep Water induced by abyssal mixing. *Universität Bremen*. Bremen 2004.
- [41] Logemann K. *Modelluntersuchung zur Erwärmung des Bodengewässers der Grönlandsee*. Universität Hamburg. Hamburg 2006.
- [42] Ronski S, Budéus G. Vertical structure reveals eddy lifetime in the Greenland Sea. *Geophys Res Lett* 2006; 33: doi:10.1029/2006GL-026045.
- [43] Kasajima Y, Olsson KA, Johannessen T, *et al.* A submesoscale coherent eddy in the Greenland Sea in 2003. *J Geophys Res C Oceans* 2006; 111: doi:10.1029/2005JC003130.
- [44] McWilliams JC. Submesoscale, coherent vortices in the ocean. *Rev Geophys* 1985; 23: 165-82.

Received: January 18, 2008

Revised: July 8, 2008

Accepted: March 5, 2009

© Budéus and Ronski; Licensee *Bentham Open*This is an open access article licensed under the terms of the Creative Commons Attribution Non-Commercial License (<http://creativecommons.org/licenses/by-nc/3.0/>) which permits unrestricted, non-commercial use, distribution and reproduction in any medium, provided the work is properly cited.